Paleoceanography and Paleoclimatology

RESEARCH ARTICLE
10.1029/2020PA003941

Stable Oxygen Isotope Composition Is Biased by Shell Calcification Intensity in Planktonic Foraminifera

M. F. G. Weinkauf[1,2], J. Groeneveld[3], J. J. Waniek[4], T. Vennemann[5], and R. Martini[1]

[1]Department of Earth Sciences, University of Geneva, Geneva, Switzerland, [2]Now at Institute of Geology and Palaeontology, Charles University, Prague, Czech Republic, [3]Helmholtz-Center for Polar and Marine Sciences, Alfred Wegener Institute, Potsdam, Germany, [4]Marine Chemistry Section, Leibniz Institute for Baltic Sea Research Warnemünde, Rostock, Germany, [5]Faculty of Geosciences and Environment, University of Lausanne, Lausanne, Switzerland

Key Points:
- $\delta^{18}O$ values in planktonic foraminiferal shells are linked with calcification intensity
- Shell calcification intensity influences buoyancy of the shells leading to variable ambient water properties
- Depth-habitat effects due to calcification intensity impact paleoenvironmental reconstructions based on foraminiferal shell geochemistry

Supporting Information:
- Supporting Information S1
- Data Set S1

Correspondence to:
M. F. G. Weinkauf,
Manuel.Weinkauf@unige.ch

Citation:
Weinkauf, M. F. G., Groeneveld, J., Waniek, J. J., Vennemann, T., & Martini, R. (2020). Stable oxygen isotope composition is biased by shell calcification intensity in planktonic foraminifera. *Paleoceanography and Paleoclimatology*, *35*, e2020PA003941. https://doi.org/10.1029/2020PA003941

Received 7 APR 2020
Accepted 14 OCT 2020
Accepted article online 17 OCT 2020

Abstract Planktonic Foraminifera are widely used for environmental reconstructions through measurements of their shell's geochemical characteristics, including its stable oxygen and carbon isotope composition. Using these parameters as unbiased proxies requires a firm knowledge of all potential confounding factors influencing foraminiferal shell geochemistry. One such parameter is the shell calcification intensity (shell weight normalized for shell size) that may influence the shell $\delta^{18}O$ value either bioenergetically (by reducing energy available and required for equilibrium isotope fractionation during faster calcification) or kinetically (by influencing calcification depth through the shell's density contrast with seawater). Specimens from the *Globigerinoides ruber*/*elongatus* complex from a sediment trap in the North Atlantic have been used to quantify the influence of shell calcification intensity on shell $\delta^{18}O$ values. Shell calcification intensity was found to have a significant effect on the shell stable oxygen isotope composition in all species. Through model fitting, it is suggested that the effect size may be in a range of 1‰ to 2‰ (depending on species, depth migration, and local oceanographic conditions). We show that the confounding effect of shell calcification intensity on stable oxygen isotope composition can be of importance, depending on the anticipated precision of the derived reconstructions. A framework is provided to quantify this effect in future studies.

1. Introduction

Planktonic Foraminifera are an abundant protist group in the world's oceans, and their calcitic shells are commonly preserved in the sediment (Schiebel, 2002; Schiebel & Hemleben, 2017). For this reason, planktonic foraminiferal shells are abundantly used for paleoenvironmental reconstructions and biomonitoring purposes (e.g., Consolaro et al., 2018; Gorbarenko & Southon, 2000; Kučera, 2007; Weinkauf et al., 2016). A major application of planktonic foraminiferal shells is the use of their geochemical compositions for reconstructions of past environmental conditions (Lea, 2002; Rohling & Cooke, 2002; Ravelo & Hillaire-Marcel, 2007; Rosenthal, 2007), which also provides the basis for climate models (e.g., Ezat et al., 2016; Ganssen & Troelstra, 1987; Groeneveld et al., 2006; Ganssen et al., 2011; Hemleben et al., 1996; Henehan et al., 2016; Ivanova, 1985; Milker et al., 2013; Steph et al., 2009).

The stable isotope composition of planktonic foraminiferal shells is not in equilibrium with seawater (Spero, 1998). For instance, for the shell's stable oxygen isotope composition, a vital effect often results in a different isotopic composition compared to a composition in equilibrium with the ambient seawater (cf. Spero et al., 1991; Zeebe et al., 2008). For different species, the size of this vital effect varies, necessitating species-specific correction functions to allow reliable paleoenvironmental interpretations (Carter et al., 2017; Spero, 1998; Steinke et al., 2005; Wit et al., 2013). The interpretation of geochemical compositions of shells may even be further complicated by intrashell variations of stable isotope compositions (Vetter et al., 2013) and ontogenetic changes in shell geochemistry (Rohling et al., 2004; Shackleton et al., 1985). For the application of stable oxygen isotope compositions of planktonic foraminiferal shells, for instance for paleoclimate (e.g., Ganssen & Troelstra, 1987; Milker et al., 2013) and depth habitat reconstructions (e.g., Mortyn & Charles, 2003; van Eijden, 1995), it is necessary to understand further factors that may bias the values measured within the shells. This is especially important when applying single-shell geochemical analyses, as the geochemical variation between individual shells precipitated under comparable conditions is mostly larger

than expected and beyond the analytical error of the measurement (Groeneveld et al., 2019; Killingley et al., 1981; Schiffelbein & Hills, 1984). For instance, the seasonality of species may play an important role in the observed stable isotope composition of a temporally integrated sediment sample (Ganssen et al., 2011; King & Howard, 2005). Another problem can occur in the case of pseudo-cryptic speciation, when two distinct species are not differentiated although they have varying geochemical shell compositions, as was shown for instance for *Globigerinoides ruber* (white) and *Globigerinoides elongatus* (Steinke et al., 2005; Wang, 2000). While progress is being made in the understanding of individual variations of the geochemical signal in planktonic Foraminifera, a larger part of the observable variation in single-shell analyses is still unaccounted for (cf. Groeneveld et al., 2019, and citations therein). Incidentally, there have been few studies so far investigating to what degree the stable oxygen isotope composition of individual planktonic foraminiferal shells is influenced by their shell calcification intensity (the amount of calcite in the shell, normalized for shell size; Billups & Spero, 1995; Ezard et al., 2015).

Shell calcification intensity varies widely across planktonic foraminiferal species and can in its own right be used as an environmental proxy (cf. Marshall et al., 2013; Weinkauf et al., 2016). In this regard, shell calcification intensity has been mostly used as a proxy for dissolution (Broecker & Clark, 2001; Lohmann, 1995; Schiebel et al., 2007) and marine carbonate system variables (Bijma et al., 1999, 2002; de Moel et al., 2009; Davis et al., 2019; Osborne et al., 2016; Spero et al., 1997; Weinkauf et al., 2013). However, other studies could show that the picture is more complicated and shell calcification intensity is indeed influenced by a variety of environmental factors (Aldridge et al., 2012; Marshall et al., 2013; Mohan et al., 2015; Weinkauf et al., 2016), which may also have an influence on the shell's geochemical composition (e.g., water temperature and salinity; Davis et al., 2016; Gonzalez-Mora et al., 2008; Zarkogiannis et al., 2019).

The mechanisms of shell calcification in Foraminifera are still a matter of discussion, with seawater vacuolization, transmembrane ion transport, calcification via organic matrices, and active pH manipulation all touted as possibly valid calcification models (de Nooijer et al., 2009, 2014; Ohno et al., 2016; Toyofuku et al., 2017). In this regard, transmembrane ion transport employs active ion transport between the seawater and cytoplasm to compose calcite crystals. In contrast, the other processes support calcification by either limiting (and potentially concentrating) the volume of seawater solution from which to calcify (seawater vacuolization) or by changing the framework parameters (providing a crystallization matrix and lowering the pH) under which to calcify. Since shell calcification in Foraminifera is complicated and not fully understood, only comparatively little work has been performed so far to investigate its influence on the shell geochemical composition (e.g., Raitzsch et al., 2010; Steinhardt et al., 2015; Ushikawa et al., 2015; van Dijk et al., 2017; Watson, 2004; Yu et al., 2018). Nevertheless, it is feasible that calcification intensity of the shell can affect the foraminiferal shell's geochemical composition via two potential pathways.

The first possible influence stems from the calcification process itself. Normally, organisms preferentially use lighter isotopes of elements for inclusion in their organic and inorganic structural parts when compared to inorganic calcite (De La Rocha, 2003; Gabitov et al., 2012; Kendall & Caldwell, 1998). This is because inclusion of lighter isotopes is energetically favored, since chemical bonds are weaker (Kendall & Caldwell, 1998). In this regard, the calcification process involves an active selection of isotopes from the seawater, which is normally considered to be the so-called vital effect (fractionation). This process is time and energy consuming, especially when active membrane transport of components is required (de Nooijer et al., 2014; Toyofuku et al., 2017). Under the assumption that a higher calcification intensity in the adult foraminiferal shell was derived from a faster calcification (instead of longer calcification at a constant rate) during chamber formation (Hemleben et al., 1987; Spero, 1988; Spero et al., 1991), we may assume that this must increase the size of the vital effect. This is because this scenario leaves the foraminifer with less time to perform the calcification process, necessitating a more frequent inclusion of the much more abundant lighter isotope ^{16}O and thus lower $\delta^{18}O$ values of the shell when the shell's calcification intensity increases (Norris, 1998). Such a process has for instance been observed in corals, where faster growing parts of the skeletal structure were enriched in ^{16}O (McConnaughey, 1989).

The second influence stems from the effect of a heavier shell on the depth habitat of the foraminifer. While planktonic foraminiferal species in general have a certain, species-specific preference for water column conditions (Bé, 1977; Bé & Tolderlund, 1971; Numberger et al., 2009; Schiebel & Hemleben, 2017; Weiner et al., 2012), this habitat has been shown to be inclusive of a wide and flexible range of water column

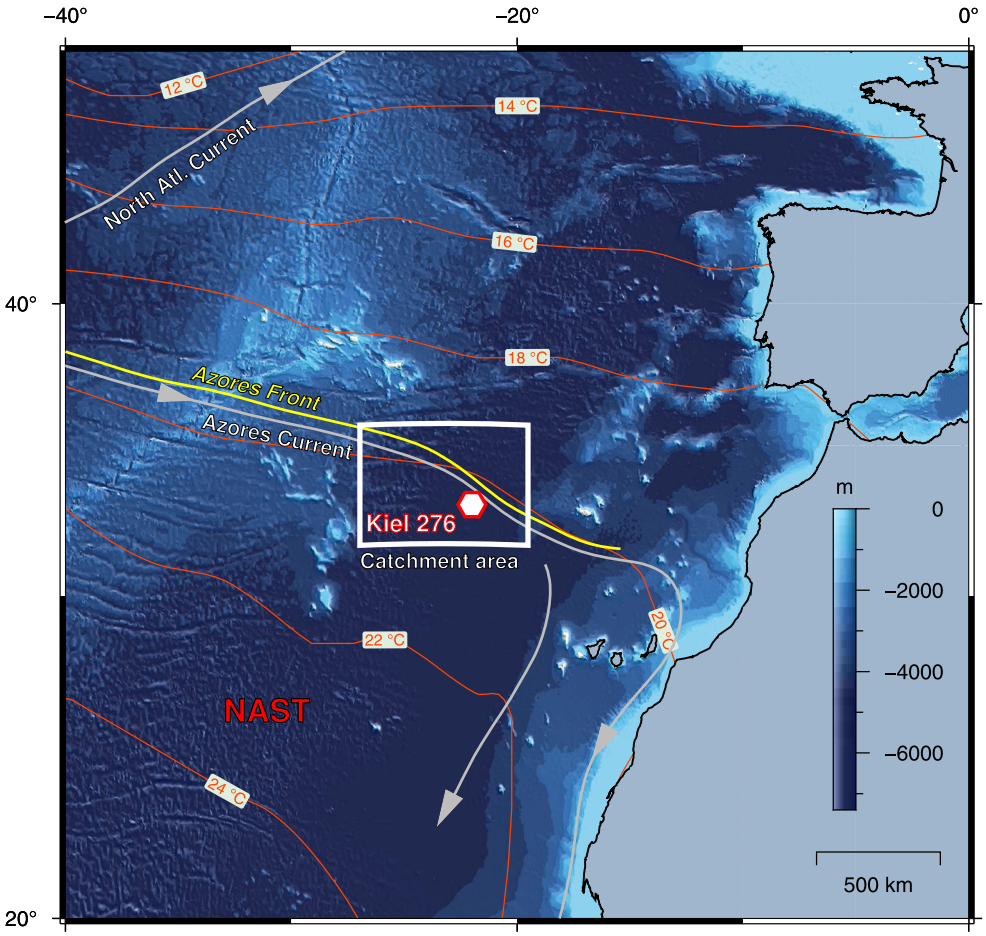

Figure 1. Sampling area including position of the mooring Kiel 276 and the catchment area of the 2,000 m-sediment trap (Waniek et al., 2005). The Azores Front separates the North Atlantic temperate water from the North Atlantic subtropical gyre (NAST). Bathymetry from ETOPO1 (Amante & Eakins, 2009), temperature isolines from the "averaged decades" annual data set of the World Ocean Atlas 2018 (Locarnini et al., 2018).

depths (cf. Rebotim et al., 2017; Meilland et al., 2019). Moreover, there are signs for an ontogenetic change of the depth habitat in planktonic Foraminifera (Eggins et al., 2003; Schiebel & Hemleben, 2017; van Eijden, 1995). Concomitant with this ontogenetic change in depth habitat, some foraminiferal species add calcitic layers to their shell, which can increase shell weight by, for example, 28% in the case of *Trilobatus sacculifer* (Bé, 1980) and around 40% in *Globorotalia* (Schweitzer & Lohmann, 1991). It is therefore likely that planktonic foraminifers with a higher calcification intensity live deeper than lighter calcified specimens of the same species due to gravitational pull and reduced buoyancy (Haenel, 1987; Weinkauf, Zwick, et al., 2020; Zarkogiannis et al., 2019). The stable isotope composition of the seawater indirectly varies as a function of density, because density is largely controlled by the salinity and temperature of the water through changes in evaporation and/or freshwater contributions. If higher density shells find themselves at greater depths than lower density shells, this could influence their $\delta^{18}O$ values. For example, foraminiferal shells with a higher shell calcification intensity would have formed within higher-salinity or lower-temperature waters at larger water depths and, thus, show increased $\delta^{18}O$ values.

In this study, we use sediment trap material from the subtropical North Atlantic to study the correlation between shell calcification intensity and the whole-shell $\delta^{18}O$ values of individual shells of planktonic Foraminifera, to quantify the influence and deduce the mechanisms leading to potential correlations with external crystallization factors. Investigating such confounding factors is of great importance to increase the mechanistic understanding of and confidence in using foraminiferal shell stable isotope geochemistry as an environmental proxy.

2. Material and Methods

2.1. Sampling Material

We used material from the 2,000 m-deep sediment trap Kiel 276-25 in the North Atlantic (33°N, 22°W; Figure 1), spanning the time between May 2005 and April 2006 with a sampling resolution of 1–2 months. We selected four of the sediment trap samples, distributed over an entire year and covering all seasons, for further analyses (Table 1). The >63 μm fraction of the dried and depoisoned sediment trap samples was desalted using MilliQ water and then dried overnight at 50°C. Desalted samples were then split into the 63–150 and >150 μm size fraction using a Retsch AS 200 sieve tower (10 min at intensity 40). Only the >150 μm size fraction was used for further analyses to avoid ontogenetic effects on calcification intensity and shell geochemistry (Blanc & Bé, 1981), as these can be assumed to be postgametogenic adult specimens (Peeters et al., 1999). All planktonic foraminiferal shells from all samples were separated from the residue. Planktonic foraminifers for shell calcification analyses were picked from representative samples of those concentrates, split with an ASC Scientific MS-1 microsplitter, such that approximately 100 specimens per sample were available for analyses. In samples with fewer specimens, 100% of the sample was used (Table 1).

All specimens for analyses were cleaned with 2% ethanol and brushes and then rinsed in distilled water and on wet filter paper. They were then transferred into 10-hole cardboard slides and left to dry at room temperature for at least 24 hr.

2.1.1. Environmental Setting

The sediment trap is located close to the Azores Front, which separates the temperate North Atlantic water from the North Atlantic subtropical gyre and is influenced by both water regimes (Figures 1 and 2; Fründt & Waniek, 2012). The following environmental data were calculated as averages for the respective sample duration and the estimated catchment area of the sediment trap (Table 1; based on Waniek et al., 2000, 2005): (1) Sea surface temperature (SST) is based on the NOAA Optimum Interpolation (OI) Sea Surface Temperature (SST) V2 provided by the NOAA/OAR/ESRL PSD, Boulder, Colorado, USA (https://www.esrl.noaa.gov/psd/; Reynolds et al., 2002). Although these data only provide values from the mixed layer, they are the only data with sufficient temporal resolution available for the specific time intervals analyzed here, which should not impact the analyses to any noteworthy extend since the chosen species (see below) are all surface dwellers. (2) Sea surface salinity (SSS) was calculated from the EN4 quality controlled ocean data (v. EN4.2.0; Good et al., 2013). (3) The carbonate system of the seawater was estimated using the MS Excel program CO2Sys v. 2.1 (Lewis et al., 1998) with K1 and K2 constants from Mehrbach et al. (1973) (refit by Dickson & Millero, 1987) and KSO4 constant after Dickson (1990). (4) While planktonic Foraminifera show a vital effect in their shell $\delta^{18}O$ values, their shell isotopic composition is not independent of the $\delta^{18}O$ of the sea water. We thus used the data set of LeGrande and Schmidt (2006) to estimate annual and spatial variations of $\delta^{18}O_{Seawater}$ within the uppermost 100 m of the water column within the catchment area of the sediment trap.

2.1.2. Choice of Species

The species were chosen to fulfill certain criteria as following: (1) They had to have a relatively restrictive depth habitat, so that our environmental reconstructions were effective in eliminating confounding factors but still large enough to observe habitat depth changes. (2) They needed to be abundant enough for a reliable analysis. (3) They had to be species which are often used in geochemical analyses to maximize the practical value of the study and stay comparable with the literature.

We thus selected the three species *Globigerinoides ruber* (pink), *Globigerinoides ruber* (white), and *Globigerinoides elongatus* (Figure 3). They all have photosymbionts (Schiebel & Hemleben, 2017) and are, thus, restricted to the photic zone, as is also confirmed by in situ studies from the North Atlantic (Lessa et al., 2019; Meilland et al., 2019; Rebotim et al., 2017; Richey et al., 2019; Thirumalai et al., 2014). *Globigerinoides elongatus* lives somewhat deeper (around 40–60 m) than *G. ruber* (around 20–40 m) (Lessa et al., 2019; Meilland et al., 2019), with *G. ruber* (pink) potentially preferring an even shallower habitat than *G. ruber* (white) due to an increased demand for sunlight to enable photosynthesis (Rebotim et al., 2017). All species prefer relatively warm habitats and are globally distributed in the tropical and subtropical regions (Siccha & Kučera, 2017). *Globigerinoides ruber* (pink) and, to a lesser extent, *G. elongatus* seem to be indicative for even warmer waters (Bonfardeci et al., 2018; Jentzen et al., 2019). *Globigerinoides ruber* could further

Table 1
Sample Metadata for Material From Sediment Trap Kiel 276-25 and Number of Specimens of Globigerinoides ruber (Pink), Globigerinoides ruber (White), and Globigerinoides elongatus Used for Analyses

Sample	Start	End	Dur.	SST	SSS	*G. ruber* (pink)	*G. ruber* (white)	*G. elongatus*
1	2005-05-01	2005-07-01	61	20.95	36.63	27 (19)	60 (11)	38 (13)
3	2005-09-01	2005-11-01	61	22.93	36.76	55 (21)	92 (7)	75 (12)
5	2006-01-01	2006-02-01	31	18.25	36.65	2 (2)	70 (12)	34 (13)
7	2006-03-01	2006-04-01	31	18.23	36.58	0 (0)	34 (12)	41 (14)

Note. Number of specimens used for shell calcification intensity analyses and (in parentheses) how many of these were used for geochemical analyses. Only results for the latter are presented here. Start = start date of sampling; End = end date of sampling; Dur. = sampling duration (d); SST = sea surface temperature (°C; Reynolds et al., 2002); SSS = sea surface salinity (Good et al., 2013).

be shown to be euryhaline, making it adaptable to environments which deviate from normal open-ocean conditions (Bijma et al., 1990).

All three species are extensively used in geochemical analyses, and especially, *G. ruber* (white) and *G. elongatus* were studied in detail concerning their differences in geochemical shell composition (Carter et al., 2017; Kawahata, 2005; Numberger et al., 2009; Steinke et al., 2005; Wang, 2000). In earlier studies, *G. ruber* (white) and *G. elongatus* were considered phenotypes of the same species (often called *G. ruber* sensu stricto and *G. ruber* sensu lato), but it was shown by Aurahs et al. (2011) that all three are indeed distinct species.

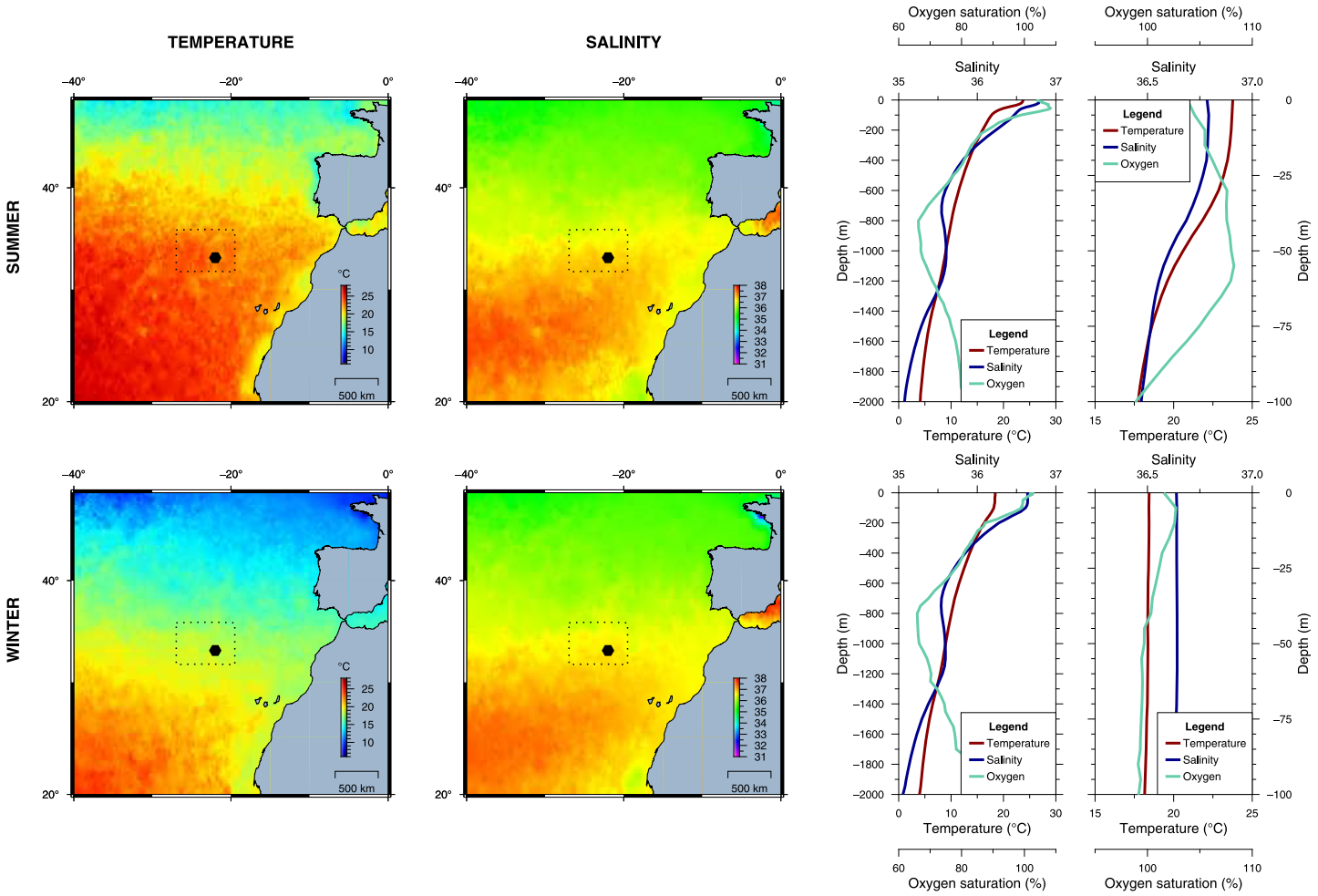

Figure 2. Oceanography of the sampling area during summer and winter. Maps showing sea surface temperature and salinity as average of the upper 50 m of the water column. Depth profiles showing average values for the catchment area of the trap (indicated by the dotted rectangle in the maps) for the upper 2,000 m (depth of the sediment trap) and upper 100 m (maximum living depth of the selected foraminiferal species). Temperature and salinity data from the 2005–2017 "decadal period" and oxygen as "average over all decades" of the World Ocean Atlas 2018 (Garcia et al., 2018; Locarnini et al., 2018; Zweng et al., 2018).

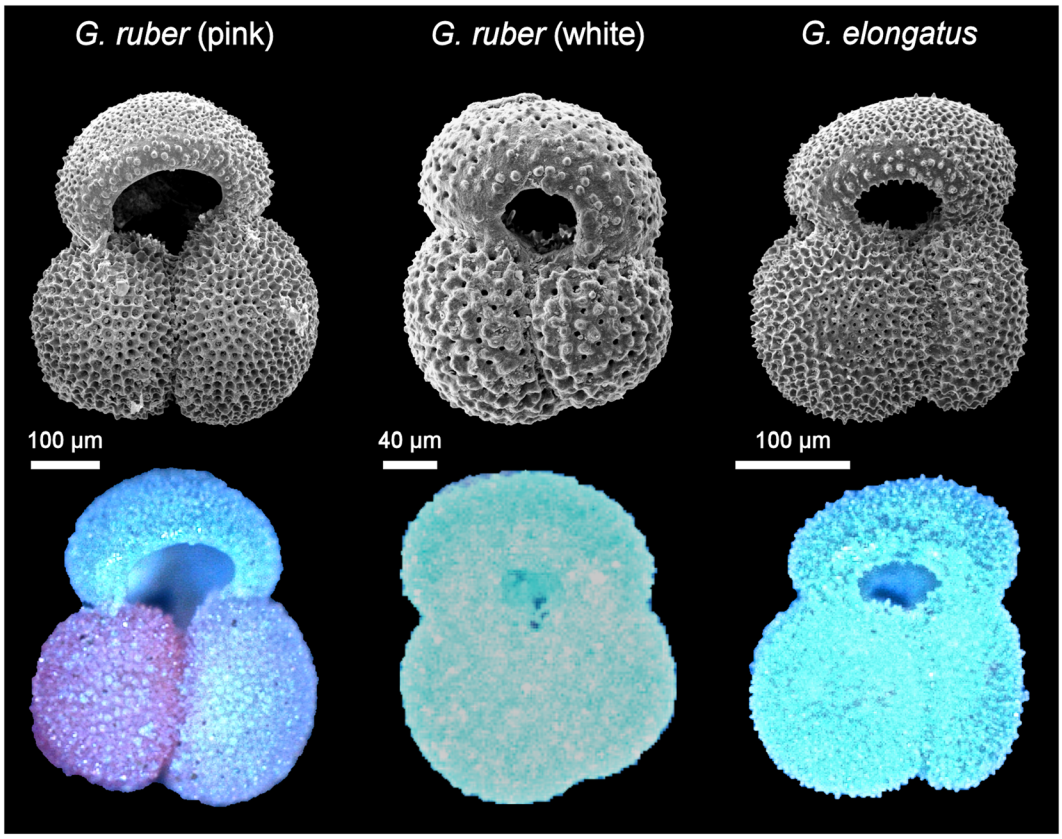

Figure 3. Depiction of the three planktonic foraminiferal species used in this study (upper row: scanning electron micrographs; lower row: light microscopy images of the same specimens). *Globigerinoides ruber* (pink) is characterized by a reddish color of the chambers (often missing in the last and sometimes the penultimate chamber). *Globigerinoides ruber* (white) and *Globigerinoides elongatus* can be distinguished by the former having round and inflated chambers while in the latter the final and penultimate chamber are distinctly flattened and asymmetrical (Aurahs et al., 2011).

We here follow the suggestions by Aurahs et al. (2011) to distinguish *G. ruber* (white) and *G. elongatus*: *Globigerinoides elongatus* has a flat last and penultimate chamber, and especially, the last chamber is very asymmetrical, while these chambers are inflated and symmetrical in *G. ruber* (white). The separation into *G. ruber* (white) and *G. elongatus* was entirely done by the same scientists (principal author) to avoid any influence of competing species concepts. It must be noted that even within these morphospecies, cryptic diversity persists (with the exception of the monospecific *G. ruber* [pink]; Aurahs et al., 2011) and that cryptic species can differ in their shell geochemical composition (e.g., in the case of *Globigerina bulloides*; Sadekov et al., 2016). We note, however, that Darling and Wade (2008) only found one cryptic species each of *G. ruber* (white) and *G. elongatus* in our study region, eliminating the problem in our study.

2.1.3. Calcification Intensity Analysis

All specimens where weighed individually on a Mettler Toledo UMX 2 microbalance (nominal precision 0.1 µg). The empty weighing boats (Elemental Microanalysis D5007) were first weighed 10 times to reliably determine their weight. Afterward, individual foraminiferal shells were transferred into the weighing boats and weighed four times each, and the difference between the empty and filled weighing boat was noted as the weight (W) of the foraminifer. The replication of weighing per individual allows to determine the measurement error of the weighing procedure.

The same specimens were then photographed in apertural standard view at 27.5 × magnification on a Leica M420 light microscope using a Leica DFC420 camera. The cross-sectional area (A) of each foraminifer was extracted in FIJI (Schindelin et al., 2012) running ImageJ v. 1.52o (Schneider et al., 2012), and the

calcification intensity was calculated as area density $\rho_A = \frac{W}{A}$ sensu Marshall et al. (2013) (cf. Figure S1 in the supporting information).

An additional set of specimens was investigated under the scanning electron microscope (SEM), using a JEOL JSM7001F analytical thermal field emission SEM with a Schottky electron gun, to check the foraminifers for any signs of dissolution. Specimens chosen for this procedure were mounted on SEM stubs using adhesive carbon pads and sputtered with gold. All specimens were first photographed from the outside to examine their shell surface. They were then cracked open with the help of a needle, and (after renewed gold sputtering) the shell microstructure was investigated in the cross sections of the shell's fragments.

2.1.4. Stable Isotope Analyses

Approximately 50 specimens in total per species for stable isotope analysis were selected using a stratified random sampling approach. For this, the sample was divided into four so-called strata based on the range of measured calcification intensities, such that each stratum would span $\frac{1}{4}$ of the observed calcification intensity range. An equal number of specimens was then randomly selected from each stratum, so that our samples would cover the entire calcification intensity range without being biased toward more frequently occurring calcification intensities. Only these randomly selected specimens were the basis for all results presented in this study. All ensuing geochemical measurements were performed at the Faculty of Geosciences and Environment of the University of Lausanne. Selected specimens were individually cleaned via sonication (3 min) in Krantz cells filled with tap water to remove any potential contaminants from the handling during the calcification intensity analysis. Individual specimens were then transferred into glass vials, closed with screw-on septum caps, and then analyzed for their $\delta^{13}C$ and $\delta^{18}O$ values on a Gas Bench II He-carrier gas system connected to a ThermoFisher DeltaPlus XL mass spectrometer (method by Spötl & Vennemann, 2003, adapted for small vials of 4 ml volume: acidifying with four drops of orthophosphoric acid of a specific gravity of 1.90, and measuring only four instead of ten peaks for each sample). Carrara marble was used as a standard and was measured alongside the foraminiferal shells every six samples and additionally two times at the start and at the end of each sequence. Foraminiferal shells were arranged along the measurement sequence by weight, so that standards could be prepared to have a comparable weight to the surrounding samples and, hence, yields for the carbonate were equal. All values are expressed in the familiar δ-notation and normalized against NBS-19 on the VPDB-scale. Repeated measurements for the standards after a size correction are within 0.1‰ for both oxygen and carbon isotope compositions.

2.2. Data Analysis

All data analyses were performed in R v. 3.6.2 (R Core Team, 2019) and interpreted following Murthaugh (2014). Differences between parameters across species were tested using pairwise Mann-Whitney *U* tests (Mann & Whitney, 1947) with *p* values corrected for the false discovery rate after Benjamini and Yekutieli (2001). The correlation between selected variables was tested using Kendall rank-order correlation (Kendall, 1938). The data for regression analyses were cleaned from potential outliers using bagplots of $\delta^{18}O$ against ρ_A (Rousseeuw et al., 1999) as implemented in the R-package "aplpack" v. 1.3.3. Problems with multicollinearity in the data were eliminated following suggestions by Dormann et al. (2013): (1) The presence of a considerable degree of multicollinearity in the data was tested based on the condition number (Dormann et al., 2013). (2) Multicollinearity clusters in the predictor variables were identified using principal component analysis (PCA; Booth et al., 1994) and cluster analysis on Hoeffding's *D*-similarity index (Hoeffding, 1948; Kauffmann & Rousseeuw, 2009). (3) The ranking of collinear parameters was established based on the deviance in bivariate regressions with $\delta^{18}O$ values. (4) Sequential regression (Graham, 2003) was used to calculate the residuals of lower-ranked parameters, and we used these as new parameters for the ensuing analyses (Dormann et al., 2013). We further applied general additive models (GAM; Friedman & Stuetzle, 1981) to identify all factors influencing the $\delta^{18}O$ values of the foraminiferal shells in the R-package "gam" v. 1.16.1 and tested the significance of the influence of shell calcification intensity via analysis of variances (ANOVA; Fisher, 1919) of the additive model against a null model without calcification intensity. When the shell calcification intensity had a significant effect when accounting for all other parameters, the relationship between ρ_A and shell $\delta^{18}O$ values was modeled using linear and nonlinear regressions (Bolker, 2008). We tried the following regression functions: (1) a Michaelis-Menten (Michaelis & Menten, 1913) function and (2) a power law function—both are rooted in

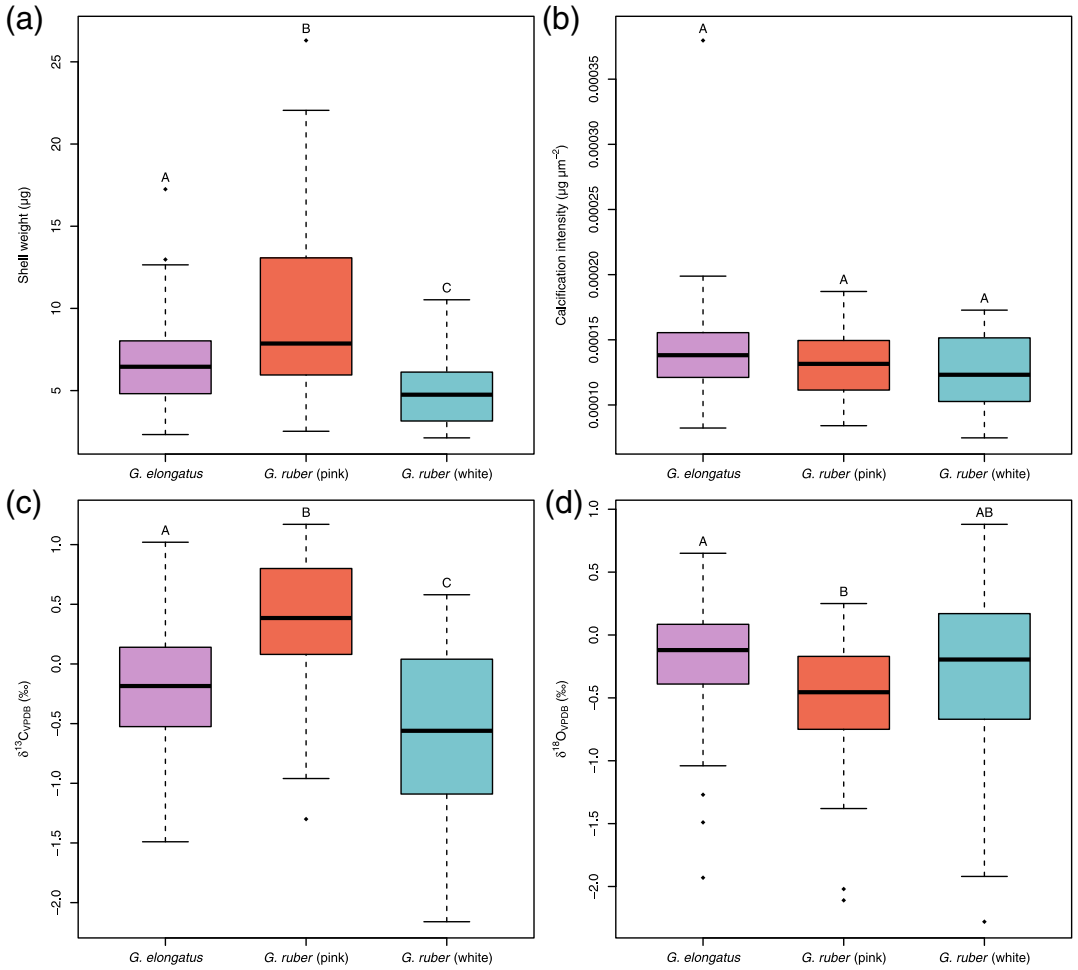

Figure 4. Comparison of shell weight (a), shell calcification intensity (b), and shell $\delta^{13}C$ (c) and $\delta^{18}O$ (d) values of shells of *Globigerinoides ruber* (pink), *Globigerinoides ruber* (white), and *Globigerinoides elongatus* from sediment trap Kiel 276-25. Thick lines indicate median, boxes cover interquartile range (IQR), whiskers extend to 1.5 × IQR, and outliers are marked by black diamonds. Uppercase letters above the boxes denote groups according to pairwise Mann-Whitney *U* tests.

bioenergetic assumptions of cell biology and would thus be suitable candidate functions under the assumption that the energy-consuming process of shell calcification leaves its imprint in the observed ρ_A-$\delta^{18}O$ relationship by limiting the potential for isotope fractionation (Russell et al., 2004; Raitzsch et al., 2010)—(3) a monomolecular function and (4) a second-degree polynomial function, which are functionally suitable to describe the fractionation process of isotopes during calcification (Groeneveld et al., 2018; Pearson, 2012; Steinhardt et al., 2015). Because most of the equations of the fitted models can only describe relationships in the first quadrant (to avoid, e.g., division by zero), 10‰ had been added to all $\delta^{18}O$ values to transform them into positive values for this step. The corrected Akaike information criterion (AIC_c; Akaike, 1974) in combination with Akaike weights (Wagenmakers & Farrell, 2004) was used to determine the best fitting model and the effect size (the amount of change in $\delta^{18}O$ caused by the variation of ρ_A) was estimated from the regressions. The relationship between $\delta^{18}O$ and $\delta^{13}C$ was investigated using a Deming regression (Deming, 1943) that took the associated measurement error in both values into account, using the R-package "deming" v. 1.4.

3. Results

We analyzed the shell calcification intensity and shell geochemical composition of 136 specimens of the *Globigerinoides ruber*/*elongatus* complex from four samples representative of an entire year from sediment

Table 2
Measured Mean Foraminiferal Shell Parameters of Three Species of Planktonic Foraminifera From Sediment Trap Kiel 276-25

Species	D	W	ρ_A	$\delta^{13}C$	$\delta^{18}O$
Globigerinoides ruber (pink)	334.2	10.15	1.31	0.334	-0.533
Globigerinoides ruber (white)	240.8	4.90	1.26	-0.588	-0.363
Globigerinoides elongatus	273.5	6.89	1.43	-0.215	-0.206

Note. D = shell Feret diameter (μm); W = shell weight (μg); ρ_A = shell calcification intensity (1×10^4 μg μm^{-2}); $\delta^{13}C$ = Vienna Pee Dee Belemnite stable carbon isotopes, normalized against NBS-19; $\delta^{18}O$ = Vienna Pee Dee Belemnite stable oxygen isotopes, normalized against NBS-19.

trap Kiel 276-25 (Figure S2; Table 1). In total, 42 specimens of *Globigerinoides ruber* (pink), 42 specimens of *Globigerinoides ruber* (white), and 52 specimens of *Globigerinoides elongatus* were successfully analyzed. The results have been summarized in Figure 4 and Table 2.

In terms of shell weight, we note that specimens of *G. ruber* (pink) are on average more than twice as heavy as specimens of *G. ruber* (white) and more than 25% heavier than *G. elongatus* specimens. The difference between all species is moderately significant at $p < 0.02$ according to pairwise Mann-Whitney U tests, indicating a general inherent difference in net shell weight. A different picture emerges when examining the shell calcification intensities, which eliminates the size differences between species on the shell weight (cf. Table 2). *Globigerinoides elongatus* is most heavily calcified, followed by *G. ruber* (pink) and *G. ruber* (white). However, these differences are all very small and insignificant at $p > 0.3$, implying a comparable size-weight ratio between the species. This suits well with the fact that they are closely related and inhabit roughly the same portion of the water column, which requires a comparable density contrast with the surrounding seawater.

For the stable isotope composition, we also see considerable differences between the species. The $\delta^{13}C$ values of *G. ruber* (pink) are positive, while they are negative for the other species, with *G. ruber* (white) having the lowest values. The difference in average $\delta^{13}C$ values is moderately significant for all pairwise comparisons ($p < 0.02$). For the stable oxygen isotopes, we see another signal. Values are highest for *G. elongatus* and lowest for *G. ruber* (pink), but the differences between neither *G. ruber* (pink) and *G. ruber* (white) ($p = 0.131$) nor *G. ruber* (white) and *G. elongatus* ($p = 1.000$) are significant. Only between *G. elongatus* and *G. ruber* (pink) do differences in $\delta^{18}O$ values of the shell accumulate to a convincingly significant signal ($p = 0.002$).

We applied GAMs to evaluate the influence of shell calcification intensity on the stable oxygen isotope composition of shells within the *Globigerinoides ruber*/*elongatus* complex. We needed to disentangle the influence of shell calcification intensity from the effects of water temperature, salinity, and symbiont-photosynthetic activity (approximated by shell $\delta^{13}C$ values), which all influence the $\delta^{18}O$ values of foraminiferal shells. To evaluate the calcification intensity effect size, we needed to perform the analyses over a realistic range of environmental conditions. The between-sample environmental variation needed to be large enough so that the unknown within-sample variation (caused by spatial variations within the catchment area of the trap and temporal variations during the 1–2 months sampling intervals) was negligible. To do this, we used the model described in Equation 1 on the four samples in unison, so that the environmental variation was representative of an entire year and, thus, exhibited a realistic amount of variation.

$$\delta^{18}O = \ell(T) + \ell(S) + \ell(a_P) + \ell(\rho_A) + \epsilon, \quad (1)$$

with T as sea surface temperature, S as sea surface salinity, a_P as photosynthetic activity, ρ_A as shell calcification intensity, ϵ as error term, and ℓ indicating a LOESS smooth.

To facilitate the analysis of the impact of environmental factors and shell calcification on the isotopic composition of the foraminiferal shells, it was necessary to establish the multicollinearity between the different parameters included in Equation 1 in order to remove confounding factors from the analyses. We tested the presence of multicollinearity between any of the parameters by calculating the condition number of the correlation matrix as $\kappa = 11.11$, far in excess of the suggested threshold of $\kappa \geq 5$ that would imply the presence of

Table 3
Results of an Additive Model Analysis of Stable Oxygen Isotope Composition Against Temperature (T), Salinity (S), Photosynthetic Activity (a_P), and Shell Calcification Intensity (ρ_A) in Foraminiferal Shells From Sediment Trap Kiel 276-25

	Parametric terms			Nonparametric terms	
Parameter	Mean squares	*F* value	*p* value	*F* value	*p* value
Globigerinoides ruber (pink)					
a_P	4.10	44.58	<0.001	3.48	0.023
ρ_A	0.25	2.69	0.111	5.03	0.006
Globigerinoides ruber (white)					
T	61.36	371.03	<0.001	20.90	<0.001
S	1.59	9.61	0.004	21.00	<0.001
a_P	26.83	162.22	<0.001	0.81	0.487
ρ_A	5.66	34.25	<0.001	2.12	0.130
Globigerinoides elongatus					
T	48.59	536.71	<0.001	200.39	<0.001
S	0.00	0.00	0.989	97.95	<0.001
a_P	1.57	17.34	<0.001	1.84	0.144
ρ_A	0.75	8.32	0.007	0.98	0.414

collinearity. An ensuing PCA, where elements which show a loading $L > 0.3$ on the first principal component (PC) are supposed to be collinear, suggests a noteworthy collinearity between temperature $(L_{\mathrm{PC1}} = 0, ., 68)$, salinity ($L_{\mathrm{PC1}} = 0.65$), and photosynthetic activity ($L_{\mathrm{PC1}} = 0.33$). A cluster analysis (complete linkage) on the Hoeffding *D*-similarity index supports this collinearity, with only shell calcification intensity showing a similarity below 0 with the other parameters (Figure S3).

To eliminate the collinearity between temperature, salinity, and photosynthetic activity before calculation of the general additive models, we used general linear regression to regress collinear parameters against δ^{18}O as dependent variable. Through the deviance *d* of these regressions, we could establish the relative importance of the parameters on the δ^{18}O of the foraminiferal shells as (1) temperature ($d = 45.36$), (2) photosynthetic activity ($d = 42.81$), and (3) salinity ($d = 42.35$). Through sequential regression using general linear models, we then calculated the residuals for photosynthetic activity and salinity for use in the additive models instead of the raw values of these parameters. Based on these corrections for multicollinearity, the additive models we calculated (based on Equation 1) are described in Equation 2.

$$\delta^{18}\mathrm{O} = \ell(T) + \ell(e_{T + a_P}(S)) + \ell(e_T(a_P)) + \ell(\rho_A) + \epsilon, \tag{2}$$

with *e* as residuals and other parameters as for Equation 1.

Results of the GAMs according to Equation 2 are summarized in Table 3. For *G. ruber* (pink), no outliers were detected, so that we could use the entire data set for further analyses. However, we encountered the problem that because one sample did not contain any specimens, the data set was not suitable for an additive model approach because it had only three distinct temperature and salinity values. We thus limited the analyses to the photosynthetic activity and calcification intensity parameters in this species. The model suggests an influence of shell calcification intensity on shell δ^{18}O values and a significant increase in model fit when adding shell calcification intensity in comparison with the model that ignores it ($p = 0.031$). Ultimately, we can use the results from the other species to get a clearer picture of the influence of shell calcification intensity on the stable oxygen isotope composition of the foraminiferal shells considering all other parameters, even though this was impossible in *G. ruber* (pink). In *G. ruber* (white), no outliers were detected, allowing to use all data points for the analysis. Using an additive model, we could identify that all included parameters have a moderately to convincingly significant influence on the shell δ^{18}O values. An ANOVA against the null model confirms the significant increase in model fit when shell calcification intensity is included at $p < 0.001$. In *G. elongatus*, two specimens (Specimen 77 from Sample 3 and Specimen 88 from Sample 5) were identified as outliers and removed from further analyses. The GAM confirms a convincingly significant influence of temperature, photosynthetic activity, and calcification intensity, but not salinity, on the stable oxygen isotope composition of the shells. The inclusion of ρ_A improves the model significantly in

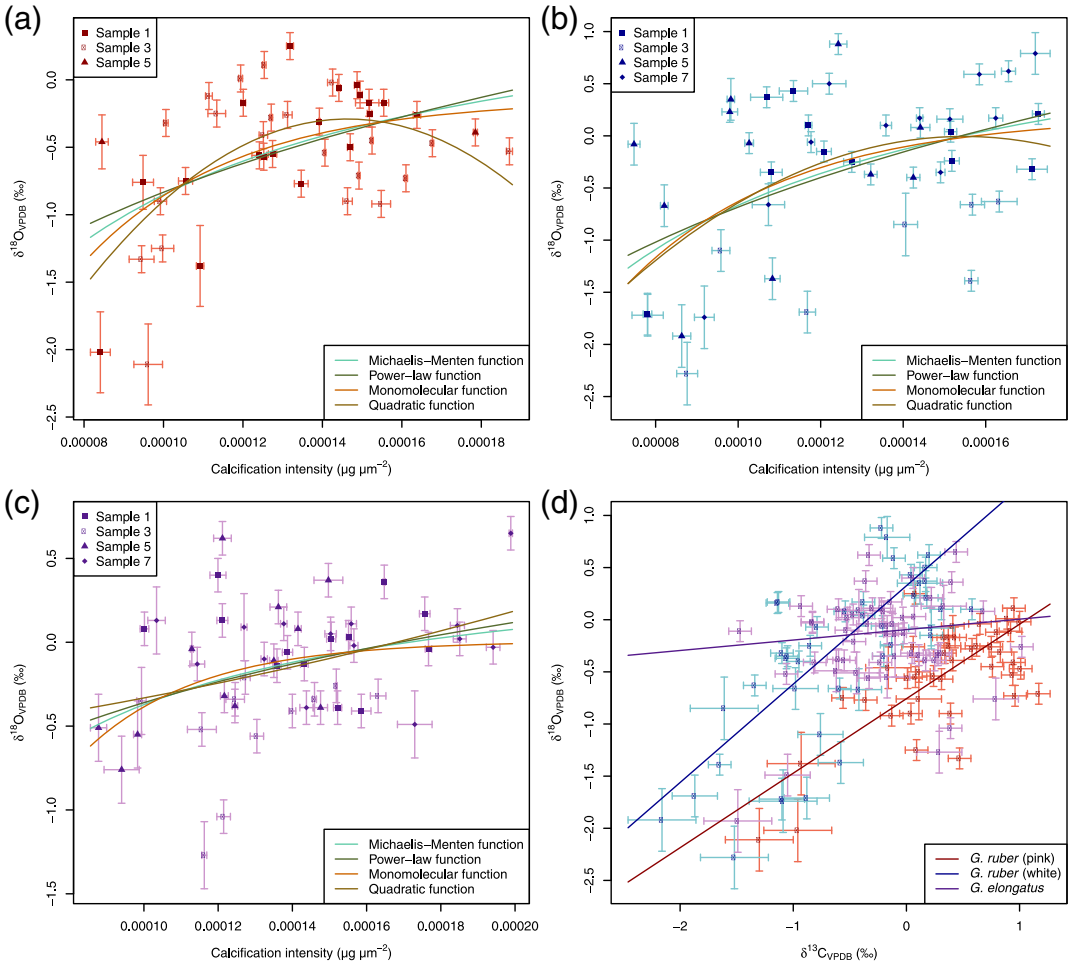

Figure 5. Models for the shell $\delta^{18}O$ values depending on the shell calcification intensity in the planktonic foraminifers (a) *Globigerinoides ruber* (pink), (b) *Globigerinoides ruber* (white), and (c) *Globigerinoides elongatus* from sediment trap Kiel 276-25. (d) Relationship between shell $\delta^{13}C$ and $\delta^{18}O$ in the same samples. Error bars indicate standard error of the measurements.

comparison to the null model ($p = 0.049$). In all species analyzed here, we thus find a significant influence of shell calcification intensity on the shell $\delta^{18}O$ values when accounting for all other relevant parameters.

4. Discussion

Our data showed a moderate collinearity with a condition number of $\kappa \approx 11$, which is a collinearity value in which most methods designed for this purpose work well and our chosen approach using sequential regression and GAMs is excellently suited (Dormann et al., 2013). Sequential regression may be prone to bias to a ranking of parameters that is not functionally correct (i.e., the ranking of variables is not representative of their influence on the dependent variable; Graham, 2003). However, our application of the deviance of bivariate regressions to establish the ranking of variables should eliminate that problem. The fact that sea surface temperature is identified as the most important factor influencing shell $\delta^{18}O$ in planktonic Foraminifera confirms the validity of our model (Spero, 1998). We therefore conclude that multicollinearity was successfully removed from our data, allowing an unbiased analysis.

The average $\delta^{18}O$ values are negative in *Globigerinoides ruber* (pink), *Globigerinoides ruber* (white), and *Globigerinoides elongatus* in our study and are compatible with a typical foraminiferal vital effect and with a preference for lighter ^{16}O during calcification in all species. These observations support the validity of our data, indicating that the $\delta^{18}O$ values we measured are not extraordinary or biased. The general trend

Table 4
Results From a Fitting of Four Model Functions to the Influence of Shell Calcification Intensity on Shell $\delta^{18}O$ in Foraminiferal Shells From Sediment Trap Kiel 276-25

Parameter	Michaelis-Menten function	Power law function	Monomolecular function	Second-degree polynomial function
Globigerinoides ruber (pink)				
AIC_c	55.175	56.953	52.577	51.526
ΔAIC_c	3.649	5.427	1.051	0.000
Akaike weight	0.089	0.036	0.325	0.550
Globigerinoides ruber (white)				
AIC_c	94.469	95.207	93.767	96.263
ΔAIC_c	0.702	1.440	0.000	2.496
Akaike weight	0.284	0.196	0.404	0.116
Globigerinoides elongatus				
AIC_c	41.277	41.093	42.097	43.340
ΔAIC_c	0.184	0.000	1.003	2.247
Akaike weight	0.321	0.352	0.213	0.114

Note. The corrected Akaike information criterion (AIC_c; Akaike, 1974) and model weights (Wagenmakers & Farrell, 2004) are reported.

in all species is an increase in $\delta^{18}O$ (from the negative toward zero) with increasing shell calcification intensity. This trend suggests that the influence of shell calcification intensity on $\delta^{18}O$ is linked to depth habitat changes when the density contrast between the shell and ambient seawater changes. This is because if calcification intensity influences $\delta^{18}O$ values through a modification of living depths via changing density contrasts with the surrounding seawater (Weinkauf, Zwick, et al., 2020; Zarkogiannis et al., 2019), we would expect lighter individuals that live in shallower depths and thus warmer water (especially in summer, we could expect temperature changes of ~6°C within the upper 100 m of the water column; cf. Figure 2), to have lower $\delta^{18}O$ values; this is indeed noted by the present data. The spatial temperature variation within the catchment area is only ~1°C in any given season (cf. Figure 2) and could not explain the observed $\delta^{18}O$ variation in the same way. If, in contrast, faster calcification rates would limit the time or energy available for fractionation, heavier calcified individuals would show reduced $\delta^{18}O$ values because of unselected uptake of the more abundant ^{16}O (Norris, 1998). This is opposite to the pattern we observe in the data, leading us to believe that higher calcification intensities in planktonic foraminiferal shells are likely the result of a longer calcification time at a constant rate, instead of an increased calcification rate which would increase the vital effect amplitude. It could also indicate that the calcification mechanism in planktonic Foraminifera is not very time sensitive during the calcification process. If true, this would make mechanism like seawater vacuolization (where the time-dependent component of accumulating calcification solution occurs before the actual calcification) and calcification via organic matrices more likely, while mechanisms like active ion transport and pH manipulation may play a secondary role. This is even more likely under our observation that $\delta^{13}C$ values are not generally correlated with calcification intensity values in our data (only in *G. ruber* [pink] is the relationship significant at $p = 0.005$; Figure S4). Given that photosynthetic activity is an important component of the pH manipulation (cf. Rink et al., 1998), this could indicate the lack of active pH manipulation of the microenvironment in at least two of the species investigated here. The potential presence of active pH manipulation via photosynthesis in *G. ruber* (pink) could coincide with two characteristics of this species: (1) As argued by Rebotim et al. (2017), *G. ruber* (pink) seems to have a higher light demand than comparable species, which may indicate that photosynthesis plays a more integral role in this species when compared to its close relatives. (2) Rink et al. (1998) showed an influence of photsynthesis on microenvironmental pH in *Orbulina universa*, which is among the largest species of planktonic Foraminifera. Given that *G. ruber* (pink) is also considerably larger than the other two species investigated here (cf. Table 2), it can be argued that its larger size allows it to harbor more symbionts, increasing their relative importance for the calcification process.

To better understand the observed relationship between ρ_A and shell $\delta^{18}O$ values and to estimate the effect size, we fitted linear and nonlinear regressions to the data. The results of this model assessment are summarized in Figure 5 and Table 4. In *G. ruber* (pink), the data are best described by a polynomial function and second best by a monomolecular function. The estimated effect size using the two best fitting models is 0.63–1.01‰. A similar signal is obtained for *G. ruber* (white), where a monomolecular function describes the data much better than the second-best model (Michaelis-Menten function; normalized probability: 0.587). The effect size in *G. ruber* (white) is approximately in the range of 1.37–1.42‰. In *G. elongatus*, the power law and Michaelis-Menten models outperform both alternative models, indicating a smaller effect size of ~0.56‰.

We consider the measured shell geochemical composition in our data largely free from constraining influences. It is known that photosynthetic activity influences the $\delta^{18}O$ value measured in foraminiferal shells (Ezard et al., 2015; Spero, 1998; Spero & Lea, 1993) but $\delta^{13}C$ is directly scaled to photosynthetic activity or bioproductivity, and hence also to depth (e.g., Norris, 1998; Spero, 1998; Spero & Lea, 1993; Spero et al., 1991). Therefore, by including shell $\delta^{13}C$ values in our GAMs, we can test for the effect of calcification intensity on shell $\delta^{18}O$ values, regardless. A shell size effect on $\delta^{13}C$ has been noted, which does not exist for $\delta^{18}O$ to any noteworthy extent in the species used here (Ezard et al., 2015; Franco-Fraguas et al., 2011; Norris, 1998; Shackleton et al., 1985), meaning that our analyses are robust against the shell size range used in this study. Carbonate ion concentration can have an effect on stable isotope compositions of planktonic Foraminifera, especially $\delta^{13}C$ values (Spero, 1998), but the sampling region is considerably stable concerning its carbonate system. We used data from the ESTOC time series (González-Dávila, 2016a, 2016b), which is situated close to sediment trap Kiel 276 and the MS Excel program CO2Sys to estimate the carbonate system parameters. The maximum annual range of CO_3^{2-} in surface waters in the region is <50 μmol kg^{-1}, and the average range is as small as <10 μmol kg^{-1} throughout spring-autumn (Table S1), ruling out a large effect of this parameter. An additional factor would be $\delta^{18}O$ of the sea water. No data of $\delta^{18}O_{Seawater}$ for the actual time of sampling are available. However, we can use the data set by LeGrande and Schmidt (2006) to estimate the possible annual variation in $\delta^{18}O_{Seawater}$ within the catchment area. These data confirm that $\delta^{18}O_{Seawater}$ varies by a maximum of 0.28‰ within the upper 100 m, which is reduced to 0.19‰ when only considering the uppermost 50 m of the water column where the majority of calcification will take place in the selected species (Table S2). The $\delta^{18}O_{Seawater}$ is therefore far too stable to explain the change in shell $\delta^{18}O$ as we observe it in our samples. We therefore believe that a better interpretation of the data is required.

One possible solution to explain the observations would be dissolution of the shells (Broecker & Clark, 2001; Lohmann, 1995; Schiebel et al., 2007), as selective dissolution of poorly crystallized, small crystallites of calcite with a particular stable oxygen isotope composition could result in a spurious $\delta^{18}O - \rho_A$ correlation. This is unlikely, however, for the following reasons: (1) We used the same stratified random sampling applied to pick the specimens for isotope analyses to choose a second random sample per species to be investigated under the SEM. The vast majority of the shells shows good to excellent preservation, with minor recrystallization observable in only a small number of shells (Figures S5–S16). (2) This is supported by a reconstruction of the carbonate system using the ESTOC time series (González-Dávila, 2016a, 2016b). Throughout the entire sampling interval, the calcite saturation state at the surface is >4, and even at the sediment trap depth of 2,000 m, it never decreases below 1.38 at any time (Table S1). The latter value is near the lower boundary below which dissolution starts to affect shell geochemistry (Dekens et al., 2002; Regenberg et al., 2006), but not yet problematic. (3) We further note that, should dissolution play a major role, we would expect to see the inverse effect. This is because calcite that was precipitated in warmer waters has a higher Mg/Ca ratio and is generally dissolved more readily than calcite precipitated in colder waters (de Villiers et al., 2002; Rosenthal et al., 2003). Since calcite that was formed in warmer water would also have lower $\delta^{18}O$ values, this process of selective dissolution would increase the $\delta^{18}O$ values of the lighter shells, such that the pattern we observe here would have been even more pronounced if such a selective dissolution would have taken place.

The other possibility is an environmental effect. On the one hand, this could for instance be a salinity effect. Although salinity was determined as least important and nonsignificant parameter and is strongly collinear with temperature, this is only true for the remote and averaged environmental data available here. It was shown that such data often underestimate the true short-term variation in oceanic settings (Laepple &

Huybers, 2014a, 2014b). *Globigerinoides ruber* is very resistant against salinity changes (Bijma et al., 1990), and planktonic Foraminifera can build new chambers within hours (Bé et al., 1979; Spero, 1988), which would make it theoretically feasible that the local salinity could have changed sufficiently on smaller time scales (e.g., via north-south fluctuation of the Azores front; Fründt & Waniek, 2012) without influencing chamber formation in the Foraminifera, thus explaining part of the measured range of compositions. However, this is unlikely to be responsible for the majority of the correlation due to the inconceivable amplitude of salinity changes in an open-ocean setting this assumption would require. In fact, even through fluctuation of the Azores front, salinities beyond 36.2 are practically never observed in this oceanographic setting (Fründt & Waniek, 2012; Pérez et al., 2003). Temperature changes due to vertical migration, on the other hand, could explain a major part of the measured differences in isotopic compositions for shells with different calcification intensities (Rebotim et al., 2019). The depth habitat of species in the *Globigerinoides ruber*/*elongatus* complex is generally shallow, partly due to its dependence on sunlight for photosynthesis, but both living and calcification depths were shown to be reasonably variable within the uppermost 50–100 m of the water column (Lessa et al., 2019; Meilland et al., 2019; Rebotim et al., 2017; Steinhardt et al., 2015). Within the studied area, the mixed layer covers this depth in winter, with an average temperature change of only 0.3°C over the top 100 m. During summer, however, the average temperature variation across the first 100 m is ~6°C and thus large enough to explain perhaps 1.5–2‰ of the observed variation in shell δ^{18}O (cf. Figure 2). Even in winter, changes beyond the recorded mean values can occur due to the fluctuation of the Azores front across the sediment trap mooring (Fründt & Waniek, 2012).

Interestingly, δ^{13}C values can be interpreted as a water depth indicator, especially pronounced in photosymbiont-bearing Foraminifera (Spero & Williams, 1988). For this reason, one would expect to note a positive correlation between δ^{13}C and δ^{18}O in such foraminiferal assemblages, where the recorded temperature changes are at least partly related to depth migration (Norris, 1998; Spero & Williams, 1988). We see a pronounced pattern of this type in *G. ruber* (pink) and *G. ruber* (white), but a much weaker signal in *G. elongatus* for our data set (Figure 5d). Coincidentally, *G. elongatus* is also the species that shows the smallest effect size of shell calcification intensity on shell δ^{18}O values. It was shown by Steinke et al. (2005) that *G. elongatus* lives generally deeper than *G. ruber*, but because the species is still dependent on light for its photosymbionts, this implies that extensive depth migration is less of a possibility for this species, which could explain why a more stable depth habitat in *G. elongatus* is compatible with our data. We hypothesize here that the measured compositions in all species are the result of a depth migration-related temperature change (directly scaled to shell calcification intensity via density contrast with the seawater). We further hypothesize that *G. elongatus* shows the smallest effect size due to its limited depth migration. If this interpretation is true, then shell calcification intensity can be a viable proxy to reduce the bias in geochemical shell measurements of planktonic Foraminifera that is associated with habitat depth. Our study can consequently be used in the implementation of bias modeling of climate archive proxies as for instance through "Sedproxy" (Dolman & Laepple, 2018) and can help to further improve the reliability of climate reconstructions (Dolman et al., 2020). Such an interpretation is also in line with earlier observations that larger shells within some species have higher δ^{13}C values (e.g., Spero & Lea, 1993), an observation that could be replicated here with high significance ($p < 0.001$ in Kendall rank-order correlation) for all species (Figure S17). Larger shells contain more cytoplasm that has a negative density contrast to the surrounding seawater. Unless the foraminifer increases its relative shell thickness (to keep the shell calcification intensity constant), it will be subject to greater buoyant forces, reducing its depth habitat as shown by the higher δ^{13}C values of its shell. This is also implied by observations in Zarkogiannis et al. (2019), where it is shown that larger shells tend to be more buoyant because their weight does not increase at the same rate as their volume if the shell thickness remains constant. This is observed in our data as well, when testing the shell size-δ^{18}O relationship using Kendall rank-order correlation (Figure S17). We found the relationship was significant ($p \geq 0.007$) in both *G. ruber* species but insignificant in *G. elongatus* ($p = 0.344$). The observed correlation coincides with the relationship between ρ_A and δ^{18}O but is more spurious since it only captures the upward component of the buoyant force and thus excludes the mediating influence of shell wall thickness (cf. Zarkogiannis et al., 2019).

Further studies are suggested in this field, ideally involving controlled laboratory experiments, especially regarding if this effect also exists for asymbiotic Foraminifera—as is implied by Billups and Spero (1995) at least for small specimens—or species which tend to develop thick crusts (Schiebel & Hemleben, 2017,

e.g., *Globoconella inflata*, *Globorotalia crassaformis*, and *Globorotalia truncatulinoides*). If our hypothesis is true, the effect of shell calcification intensity on the stable oxygen isotope composition of foraminiferal shells through depth habitat changes is rather variable between locations and species. This means that the effect on temperature reconstructions can be small enough that for most purposes a correction for shell calcification intensity does not need to be applied but a bias of around 1°C seems feasible under certain oceanographic conditions. Such effects may be important for some studies (e.g., Dolman et al., 2020), especially in regions or species where shell calcification intensity varies more strongly and in environments with strong vertical changes in the ambient seawater environment. We presented in this study a framework to deal with this problem in the future, by quantifying shell calcification intensity of specimens intended for geochemical analyses and quantifying its effect size for data correction. Since especially the portion of the influence that is caused by depth migration will be dependent on the investigated species (theoretical range of depth habitat), observed range of calcification intensity (practical range of depth habitat), and the local oceanography, no generally applicable corrections can be suggested here. Rather, we suggest to employ species-specific analyses of the kind suggested here to arrive at correction terms for the major species of planktonic Foraminifera used as paleo-proxies. We thus suggest an implementation of this factor in bias-modeling protocols in the future (e.g., Dolman & Laepple, 2018).

5. Conclusions

Our analyses of foraminiferal species of the *Globigerinoides ruber/elongatus* complex imply that shell calcification intensity has an impact on shell $\delta^{18}O$ values and therefore has the potential to be a confounding factor in environmental reconstructions derived from stable oxygen isotope measurements of planktonic foraminiferal shells.

Our data suggest that the observed effect is mainly an environmental effect, where heavier calcified shells hypothetically occupy a deeper habitat of the water column and are thus exposed to lower temperatures of their ambient seawater. The effect size will depend on the species (range of depth habitat; cf. Rebotim et al., 2019), the range of shell calcification intensity, and the local oceanography.

We suggest using shell calcification intensity studies to evaluate and account for this effect on geochemical analyses if high-precision reconstructions are needed but argue that the effect is probably small enough to not interfere with the majority of practical applications. We suggest further studies in this field and an implementation of this bias in standard bias-modeling protocols.

Acknowledgments

We thank Howard J. Spero (University of California, Davis, USA) for discussions about vital effects in planktonic Foraminifera and his support in securing funding by the Palaeontological Association. We acknowledge Urs Schaltegger (University of Geneva, Switzerland) for providing access to their work group's microbalance. Agathe Martignier (University of Geneva, Switzerland) is thanked for her help with scanning electron microscope work. Geochemical analyses of the foraminiferal shells were partly funded by a Sylvester-Bradley Award of the Palaeontological Association (granted to M. F. G. W., Reference No. PA-SB201705), which is thankfully recognized. J. J. W. is thankful for receiving funding for the work on the mooring Kiel 276 from the Deutsche Forschungsgemeinschaft (Grant Numbers WA2175/1-1, WA2175/2-1 to WA2175/3-1 and WA2157/4). We are thankful for the comments of two anonymous reviewers, who helped to greatly improve the manuscript.

Data Availability Statement

All data necessary to replicate this work are available in Data Set S1 and through https://figshare.com/under https://doi.org/10.6084/m9.figshare.12090630 (Weinkauf, Groeneveld, et al., 2020) (Creative Commons Attribution CC BY 4.0 license).

References

Akaike, H. (1974). A new look at the statistical model identification. *IEEE Transactions on Automatic Control*, *19*(6), 716–723. https://doi.org/10.1109/TAC.1974.1100705

Aldridge, D., Beer, C. J., & Purdie, D. A. (2012). Calcfication in the planktonic Foraminifera *Globigerina bulloides* linked to phosphate concentrations in surface waters of the North Atlantic Ocean. *Biogeosciences*, *9*, 1725–1739. https://doi.org/10.5194/bg-9-1725-2012

Amante, C., & Eakins, B. W. (2009). ETOPO1 1 arc-minute global relief model: Procedures, data sources and analysis(NESDIS NGDC-24). National Geophysical Data Center. http://www.ngdc.noaa.gov/mgg/global/relief/ETOPO1/docs/ETOPO1.pdf

Aurahs, R., Treis, Y., Darling, K., & Kučera, M. (2011). A revised taxonomic and phylogenetic concept for the planktonic foraminifer species *Globigerinoides ruber* based on molecular and morphometric evidence. *Marine Micropaleontology*, *79*, 1–14. https://doi.org/10.1016/j.marmicro.2010.12.001

Bé, A. W. H. (1977). An ecological, zoogeographic and taxonomic review of recent planktonic Foraminifera. In A. T. S. Ramsay (Ed.), *Oceanic micropalaeontology* (Vol. 1, pp. 1–100). London, New York, San Francisco: Academic Press.

Bé, A. W. H. (1980). Gametogenic calcification in a spinose planktonic foraminifer, *Globigerinoides sacculifer* (Brady). *Marine Micropaleontology*, *5*, 283–310. https://doi.org/10.1016/0377-8398(80)90014-6

Bé, A. W. H., Hemleben, C., Anderson, O. R., & Spindler, M. (1979). Chamber formation in planktonic Foraminifera. *Micropaleontology*, *25*(3), 294–307.

Bé, A. W. H., & Tolderlund, D. S. (1971). Distribution and ecology of living planktonic Foraminifera in surface waters of the Atlantic and Indian Oceans. In B. M. Funnell & W. R. Riedel (Eds.), *The micropalaeontology of oceans* (pp. 105–149). London: Cambridge University Press.

Benjamini, Y., & Yekutieli, D. (2001). The control of the false discovery rate in multiple testing under dependency. *The Annals of Statistics*, *29*(4), 1165–1188. https://doi.org/10.1214/aos/1013699998

Bijma, J., Faber, W. W., & Hemleben, C. (1990). Temperature and salinity limits for growth and survival of some planktonic foraminifers in laboratory cultures. *Journal of Foraminiferal Research*, *20*(2), 95–116. https://doi.org/10.2113/gsjfr.20.2.95

Bijma, J., Hönisch, B., & Zeebe, R. E. (2002). Impact of the ocean carbonate chemistry on living foraminiferal shell weight: Comment on "Carbonate ion concentration in glacial-age deep waters of the Caribbean Sea" by W. S. Broecker and E. Clark. *Geochemistry, Geophysics, Geosystems*, *3*(11), 1064. https://doi.org/10.1029/2002GC000388

Bijma, J., Spero, H. J., & Lea, D. W. (1999). Reassessing foraminiferal stable isotope geochemistry: Impact of the oceanic carbonate system (experimental results). In G. Fischer & G. Wefer (Eds.), *Use of proxies in paleoceanography: Examples from the South Atlantic* (pp. 489–512). Berlin, Heidelberg: Springer-Verlag.

Billups, K., & Spero, H. J. (1995). Relationships between shell size, thickness and stable isotopes in individual planktonic Foraminifera from 2 Equatorial Atlantic cores. *Journal of Foraminiferal Research*, *25*(1), 24–37. https://doi.org/10.2113/gsjfr.25.1.24

Blanc, P.-L., & Bé, A. W. H. (1981). Oxygen-18 enrichment of planktonic Foraminifera due to gametogenic calcification below the euphotic zone. *Science*, *213*(4513), 1247–1250. https://doi.org/10.1126/science.213.4513.1247

Bolker, B. M. (2008). *Ecological models and data in R*. New Jersey, Woodstock: Princeton University Press.

Bonfardeci, A., Caruso, A., Bartolini, A., Bassinot, F., & Blanc-Valleron, M.-M. (2018). Distribution and ecology of *the Globigerinoides ruber—Globigerinoides elongatus* morphotypes in the Azores region during the late Pleistocene-Holocene. *Palaeogeography, Palaeoclimatology, Palaeoecology*, *491*, 92–111. https://doi.org/10.1016/j.palaeo.2017.11.052

Booth, G. D., Niccolucci, M. J., & Schuster, E. G. (1994). Identifying proxy sets in multiple linear regression: An aid to better coefficient interpretation (Tech. Rep.). Washington, DC: United States Department of Agriculture.

Broecker, W., & Clark, E. (2001). An evaluation of Lohmann's Foraminifera weight dissolution index. *Paleoceanography*, *16*(5), 531–534. https://doi.org/10.1029/2000PA000600

Carter, A., Clemens, S., Kubota, Y., Holbourn, A., & Martin, A. (2017). Differing oxygen isotopic signals of *two Globigerinoides ruber* (white) morphotypes in the East China Sea: Implications for paleoenvironmental reconstructions. *Marine Micropaleontology*, *131*, 1–9. https://doi.org/10.1016/j.marmicro.2017.01.001

Consolaro, C., Rasmussen, T. L., & Panieri, G. (2018). Palaeoceanographic and environmental changes in the eastern Fram Strait during the last 14,000 years based on benthic and planktonic Foraminifera. *Marine Micropaleontology*, *139*, 84–101. https://doi.org/10.1016/j.marmicro.2017.11.001

Darling, K. F., & Wade, C. M. (2008). The genetic diversity of planktic Foraminifera and the global distribution of ribosomal RNA genotypes. *Marine Micropaleontology*, *67*, 216–238. https://doi.org/10.1016/j.marmicro.2008.01.009

Davis, A. N., Davis, C. V., Thunell, R. C., Osborne, E. B., Black, D. E., & Benitez-Nelson, C. R.(2019). Reconstructing 800 years of carbonate ion concentration in the Cariaco basin using the area density of planktonic Foraminifera shells. *Paleoceanography and Paleoclimatology*, *34*, 2129–2140. https://doi.org/10.1029/2019PA003698

Davis, C. V., Myhre, S. E., & Hill, T. M. (2016). Benthic foraminiferal shell weight: Deglacial species-specific responses from the Santa Barbara Basin. *Marine Micropaleontology*, *124*, 45–53. https://doi.org/10.1016/j.marmicro.2016.02.002

De La Rocha, C. L. (2003). Silicon isotope fractionation by marine sponges and the reconstruction of the silicon isotope composition of ancient deep water. *Geology*, *31*(5), 423–426. https://doi.org/10.1029/2001GC000200

de Moel, H., Ganssen, G. M., Peeters, F. J. C., Jung, S. J. A., Kroon, D., Brummer, G.-J. A., & Zeebe, R. E. (2009). Planktic foraminiferal shell thinning in the Arabian Sea due to anthropogenic ocean acidification? *Biogeosciences*, *6*, 1917–1925. https://doi.org/10.5194/bg-6-1917-2009

de Nooijer, L. J., Spero, H. J., Erez, J., Bijma, J., & Reichart, G.-J. (2014). Biomineralization in perforate Foraminifera. *Earth-Science Reviews*, *135*, 48–58. https://doi.org/10.1016/j.earscirev.2014.03.013

de Nooijer, L. J., Toyofuku, T., Kitazato, H., & Stanley, S. M. (2009). Foraminifera promote calcification by elevating their intracellular pH. *Proceedings of the National Academy of Sciences of the United States of America*, *106*(36), 15,374–15,378. https://doi.org/10.1073/pnas.0904306106

de Villiers, S., Greaves, M., & Elderfield, H. (2002). An intensity ratio calibration method for the accurate determination of Mg/Ca and Sr/Ca of marine carbonates by ICP-AES. *Geochemistry, Geophysics, Geosystems*, *3*(1), 1001. https://doi.org/10.1029/2001GC000169

Dekens, P. S., Lea, D. W., Pak, D. K., & Spero, H. J. (2002). Core top calibration of Mg/Ca in tropical Foraminifera: Refining paleotemperature estimation. *Geochemistry, Geophysics, Geosystems*, *3*(4), 1–29. https://doi.org/10.1029/2001GC000200

Deming, W. E. (1943). *Statistical adjustment of data*. New York: John Wiley & Sons, Ltd.

Dickson, A. G. (1990). Standard potential of the reaction: $AgCl(s)+12H_2(g) = Ag(s)+HCl(aq)$, and the standard acidity constant of the ion HSO_4^- in synthetic sea water from 273.15 to 318.15 K. *The Journal of Chemical Thermodynamics*, *22*(2), 113–127. https://doi.org/10.1016/0021-9614(90)90074-Z

Dickson, A. G., & Millero, F. J. (1987). A comparison of the equilibrium constants for the dissociation of carbonic acid in seawater media. *Deep Sea Research, Part A: Oceanographic Research Papers*, *34*(10), 1733–1743. https://doi.org/10.1016/0198-0149(87)90021-5

Dolman, A. M., Kunz, T., Groeneveld, J., & Laepple, T. (2020). Estimating the timescale-dependent uncertainty of paleoclimate records—A spectral approach. Part II: Application and interpretation. Climate of the Past Discussions.

Dolman, A. M., & Laepple, T. (2018). Sedproxy: A forward model for sediment-archived climate proxies. *Climate of the Past*, *14*(12), 1851–1868. https://doi.org/10.5194/cp-14-1851-2018

Dormann, C. F., Elith, J., Bacher, S., Buchmann, C., Carl, G., Carré, G., et al. (2013). Collinearity: A review of methods to deal with it and a simulation study evaluating their performance. *Ecography*, *36*(1), 27–46. https://doi.org/10.1111/j.1600-0587.2012.07348.x

Eggins, S., De Deckker, P., & Marshall, J. (2003). Mg/Ca variation in planktonic Foraminifera tests: Implications for reconstructing palaeo-seawater temperature and habitat migration. *Earth and Planetary Science Letters*, *212*(3–4), 291–306. https://doi.org/10.1016/S0012-821X(03)00283-8

Ezard, T. H. G., Edgar, K. M., & Hull, P. M. (2015). Environmental and biological controls on size-specific $\delta^{13}C$ and $\delta^{18}O$ in recent planktonic Foraminifera. *Paleoceanography*, *30*, 151–173. https://doi.org/10.1002/2014PA002735

Ezat, M. M., Rasmussen, T. L., & Groeneveld, J. (2016). Reconstruction of hydrographic changes in the southern Norwegian Sea during the past 135 kyr and the impact of different foraminiferal Mg/Ca cleaning protocols. *Geochemistry, Geophysics, Geosystems*, *17*, 3420–3436. https://doi.org/10.1002/2016GC006325

Fisher, R. A. (1919). The correlation between relatives on the supposition of Mendelian inheritance. *Transactions of the Royal Society of Edinburgh: Earth Sciences*, *52*(2), 399–433. https://doi.org/10.1017/S0080456800012163

Franco-Fraguas, P., Costa, K. B., & de Lima Toledo, F. A. (2011). Stable isotope/test size relationship in *Cibicidoides wuellerstorfi*. *Brazilian Journal of Oceanography*, *59*(3), 287–291. https://doi.org/10.1590/S1679-87592011000300010

Friedman, J. H., & Stuetzle, W. (1981). Projection pursuit regression. *Journal of the American Statistical Association*, *76*(376), 817–823. https://doi.org/10.1080/01621459.1981.10477729

Fründt, B., & Waniek, J. J. (2012). Impact of the Azores Front propagation on deep ocean particle flux. *Central European Journal of Geosciences*, *4*(4), 531–544. https://doi.org/10.2478/s13533-012-0102-2

Gabitov, R. I., Watson, E. B., & Sadekov, A. (2012). Oxygen isotope fractionation between calcite and fluid as a function of growth rate and temperature: An in situ study. *Chemical Geology*, *306–307*, 92–102. https://doi.org/10.1016/j.chemgeo.2012.02.021

Ganssen, G., & Troelstra, S. R. (1987). Paleoenvironmental changes from stable isotopes in planktonic Foraminifera from Eastern Mediterranean sapropels. *Marine Geology*, *75*, 221–230. https://doi.org/10.1016/0025-3227(87)90105-8

Ganssen, G. M., Peeters, F. J. C., Metcalfe, B., Anand, P., Jung, S. J. A., Kroon, D., & Brummer, G.-J. A. (2011). Quantifying sea surface temperature ranges of the Arabian Sea for the past 20000 years. *Climate of the Past*, *7*(4), 1337–1349. https://doi.org/10.5194/cp-7-1337-2011

Garcia, H. E., Weathers, K. W., Paver, C. R., Smolyar, I. V., Boyer, T. P., Locarnini, R. A., et al. (2018). Dissolved oxygen, apparent oxygen utilization, and dissolved oxygen saturation. In S. Levitus & A. Mishonov (Eds.), *World Ocean Atlas 2018, NOAA Atlas NESDIS* (Vol. 3, pp. 1–27). Silver Spring: National Oceanic and Atmospheric Administration.

González-Dávila, M. (2016a). Physical oceanography measured on water bottle samples at Site ESTOC in 2005. https://doi.pangaea.de/10.1594/PANGAEA.856610

González-Dávila, M. (2016b). Physical oceanography measured on water bottle samples at Site ESTOC in 2006. https://doi.pangaea.de/10.1594/PANGAEA.856611

Gonzalez-Mora, B., Sierro, F. J., & Flores, J. A. (2008). Controls of shell calcification in planktonic foraminifers. *Quaternary Science Reviews*, *27*(9–10), 956–961. https://doi.org/10.1016/j.quascirev.2008.01.008

Good, S. A., Martin, M. J., & Rayner, N. A. (2013). EN4: Quality controlled ocean temperature and salinity profiles and monthly objective analyses with uncertainty estimates. *Journal of Geophysical Research: Oceans*, *118*, 6704–6716. https://doi.org/10.1002/2013JC009067

Gorbarenko, S. A., & Southon, J. R. (2000). Detailed Japan Sea paleoceanography during the last 25 kyr: Constraints from AMS dating and δ^{18}O of planktonic Foraminifera. *Palaeogeography, Palaeoclimatology, Palaeoecology*, *156*(3–4), 177–193. https://doi.org/10.1016/S0031-0182(99)00137-6

Graham, M. H. (2003). Confronting multicollinearity in ecological multiple regression. *Ecology*, *84*(11), 2809–2815. https://doi.org/10.1890/02-3114

Groeneveld, J., Filipsson, H. L., Austin, W. E. N., Darling, K., McCarthy, D., Quintana Krupinski, N. B., et al. (2018). Assessing proxy signatures of temperature, salinity, and hypoxia in the Baltic Sea through Foraminifera-based geochemistry and faunal assemblages. *Journal of Micropalaeontology*, *37*(2), 403–429. https://doi.org/10.5194/jm-37-403-2018

Groeneveld, J., Ho, S. L., Mackensen, A., Mohtadi, M., & Laepple, T. (2019). Deciphering the variability in Mg/Ca and stable oxygen isotopes of individual Foraminifera. *Paleoceanography and Paleoclimatology*, *34*, 755–773. https://doi.org/10.1029/2018PA003533

Groeneveld, J., Steph, S., Tiedemann, R., Garbe-Schönberg, C.-D., Nürnberg, D., & Sturm, A. (2006). Pliocene mixed-layer oceanography for Site 1241, using combined Mg/Ca and δ^{18}O analyses of *Globigerinoides sacculifer*. *Proceedings of the Ocean Drilling Program: Scientific Results*, *202*, 1–27. https://doi.org/10.2973/odp.proc.sr.202.209.2006

Haenel, P. (1987). Intérêt paléoocéanographique d'*Orbulina universa* d'Orbigny (foraminifère). *Oceanologica Acta*, *10*(1), 15–25.

Hemleben, C., Meischner, D., Zahn, R., Almogi-Labin, A., Erlenkeuser, H., & Hiller, B. (1996). Three hundred eighty thousand year long stable isotope and faunal records from the Red Sea: Influence of global sea level change on hydrography. *Paleoceanography*, *11*(2), 147–156. https://doi.org/10.1029/95PA03838

Hemleben, C., Spindler, M., Breitinger, I., & Ott, R. (1987). Morphological and physiological responses *of Globigerinoides sacculifer* (Brady) under varying laboratory conditions. *Marine Micropaleontology*, *12*, 305–324. https://doi.org/10.1016/0377-8398(87)90025-9

Henehan, M. J., Foster, G. L., Bostock, H. C., Greenop, R., Marshall, B. J., & Wilson, P. A. (2016). A new boron isotope-pH calibration for *Orbulina universa*, with implications for understanding and accounting for 'vital effects'. *Earth and Planetary Science Letters*, *454*, 282–292. https://doi.org/10.1016/j.epsl.2016.09.024

Hoeffding, W. (1948). A non-parametric test of independence. *The Annals of Mathematical Statistics*, *19*(4), 546–557.

Ivanova, E. V. (1985). Late Quaternary biostratigraphy and paleotemperatures of the Red Sea and the Gulf of Aden based on planktonic Foraminifera and pteropods. *Marine Micropaleontology*, *9*(4), 335–364. https://doi.org/10.1016/0377-8398(85)90003-9

Jentzen, A., Schönfeld, J., Weiner, A. K. M., Weinkauf, M. F. G., Nürnberg, D., & Kučera, M. (2019). Seasonal and interannual variability in population dynamics of planktic foraminifers off Puerto Rico (Caribbean Sea). *Journal of Micropalaeontology*, *38*, 231–247. https://doi.org/10.5194/jm-38-231-2019

Kauffmann, L., & Rousseeuw, P. J. (2009). *Finding groups in data: An introduction to cluster analysis, Wiley Series in Probability and Statistics*. Hoboken, New Jersey: John Wiley & Sons, Ltd.

Kawahata, H. (2005). Stable isotopic composition of two morphotypes of *Globigerinoides ruber* (white) in the subtropical gyre in the North Pacific. *Paleontological Research*, *9*(1), 27–35. https://doi.org/10.2517/prpsj.9.27

Kendall, C., & Caldwell, E. A. (1998). Fundamentals of isotope geochemistry. In C. Kendall & J. J. McDonnell (Eds.), *Isotope tracers in catchment hydrology* (pp. 51–86). Amsterdam: Elsevier.

Kendall, M. G. (1938). A new measurement of rank correlation. *Biometrika*, *30*(1–2), 81–93. https://doi.org/10.1093/biomet/30.1-2.81

Killingley, J. S., Johnson, R. F., & Berger, W. H. (1981). Oxygen and carbon isotopes of individual shells of planktonic Foraminifera from Ontong-Java plateau, equatorial Pacific. *Palaeogeography, Palaeoclimatology, Palaeoecology*, *33*(1–3), 193–204. https://doi.org/10.1016/0031-0182(81)90038-9

King, A. L., & Howard, W. R. (2005). δ^{18}O seasonality of planktonic Foraminifera from Southern Ocean sediment traps: Latitudinal gradients and implications for paleoclimate reconstructions. *Marine Micropaleontology*, *56*(1–2), 1–24. https://doi.org/10.1016/j.marmicro.2005.02.008

Kučera, M. (2007). Planktonic Foraminifera as tracers of past oceanic environments. In C. Hillaire-Marcel, A. de Vernal, H. Chamley (Eds.), *Proxies in late Cenozoic paleoceanography, Developments in Marine Geology* (pp. 213–262). Amsterdam: Elsevier.

Laepple, T., & Huybers, P. (2014a). Global and regional variability in marine surface temperatures. *Geophysical Research Letters*, *41*, 2528–2534. https://doi.org/10.1002/2014GL059345

Laepple, T., & Huybers, P. (2014b). Ocean surface temperature variability: Large model-data differences at decadal and longer periods. *Proceedings of the National Academy of Sciences of the United States of America*, *111*(47), 16,682–16,687. https://doi.org/10.1073/pnas.1412077111

Lea, D. W. (2002). Trace elements in foraminiferal calcite. In B. K. Sen Gupta (Ed.), *Modern Foraminifera* (pp. 259–277). Dordrecht: Kluwer Academic Publishers.

LeGrande, A. N., & Schmidt, G. A. (2006). Global gridded data set of the oxygen isotopic composition in seawater. *Geophysical Research Letters*, *33*, L12604. https://doi.org/10.1029/2006GL026011

Lessa, D., Morard, R., Jonkers, L., Venancio, I. M., Reuter, R., Baumeister, A., et al. (2019). Vertical distribution of planktonic Foraminifera in the subtropical South Atlantic: Depth hierarchy of controlling factors. *Biogeosciences Discussions*, *17*, 1–29.

Lewis, E., Wallace, D., & Allison, L. J. (1998). Program developed for CO_2 system calculations (*4735*). Oak Ridge: Carbon Dioxide Information Analysis Center.

Locarnini, R. A., Mishonov, A. V., Baranova, O. K., Boyer, T. P., Zweng, M. M., Garcia, H. E., et al. (2018). Temperature. In A. Mishonov (Ed.), *World Ocean Atlas 2018, NOAA Atlas NESDIS* (Vol. 1, pp. 1–45). Silver Spring: National Oceanic and Atmospheric Administration.

Lohmann, G. P. (1995). A model for variation in the chemistry of planktonic Foraminifera due to secondary calcification selective dissolution. *Paleoceanography*, *10*(3), 445–457. https://doi.org/10.1029/95PA00059

Mann, H. B., & Whitney, D. R. (1947). On a test of whether one of two random variables is stochastically larger than the other. *The Annals of Mathematical Statistics*, *18*(1), 50–60. https://doi.org/10.1214/aoms/1177730491

Marshall, B. J., Thunell, R. C., Henehan, M. J., Astor, Y., & Wejnert, K. R. (2013). Planktonic foraminiferal area density as a proxy for carbonate ion concentration: A calibration study using the Cariaco Basin Ocean Time Series. *Paleoceanography*, *28*, 1–14. https://doi.org/10.1002/palo.20034

McConnaughey, T. (1989). ^{13}C and ^{18}O isotopic disequilibrium in biological carbonates: I. Patterns. *Geochimica et Cosmochimica Acta*, *53*(1), 151–162. https://doi.org/10.1016/0016-7037(89)90282-2

Mehrbach, C., Culberson, C. H., Hawley, J. E., & Pytcowicx, R. M. (1973). Measurement of the apparent dissociation constants of carbonic acid in seawater at atmospheric pressure. *Limnology and Oceanography*, *18*(6), 897–907. https://doi.org/10.4319/lo.1973.18.6.0897

Meilland, J., Siccha, M., Weinkauf, M. F. G., Jonkers, L., Morard, R., Baranowski, U., et al. (2019). Highly replicated sampling reveals no diurnal vertical migration but stable species-specific vertical habitats in planktonic Foraminifera. *Journal of Plankton Research*, *41*(2), 127–141. https://doi.org/10.1093/plankt/fbz002

Michaelis, L., & Menten, M. L. (1913). Die Kinetik der Invertinwirkung. *Biochemische Zeitschrift*, *49*, 333–369.

Milker, Y., Rachmayani, R., Weinkauf, M. F. G., Prange, M., Raitzsch, M., Schulz, M., & Kučera, M. (2013). Global and regional sea surface temperature trends during marine isotope stage 11. *Climate of the Past*, *9*(5), 2231–2252. https://doi.org/10.5194/cp-9-2231-2013

Mohan, R., Shetye, S. S., Tiwari, M., & Anilkumar, N. (2015). Secondary calcification of planktic Foraminifera from the Indian sector of southern ocean. *Acta Geologica Sinica (English Edition)*, *89*(1), 27–37. https://doi.org/10.1111/1755-6724.12392

Mortyn, P. G., & Charles, C. D. (2003). Planktonic foraminiferal depth habitat and $\delta^{18}O$ calibrations: Plankton tow results from the Atlantic sector of the Southern Ocean. *Paleoceanography*, *18*(2), 1037. https://doi.org/10.1029/2001PA000637

Murthaugh, P. A. (2014). In defense of p values. *Ecology*, *95*(3), 611–617. https://doi.org/10.1890/13-0590.1

Norris, R. D. (1998). Recognition and macroevolutionary significance of photosymbiosis in molluscs, corals, and Foraminifera. In R. D. Norris, & R. M. Corfield (Eds.), *Isotope paleobiology and paleoecology*, *The Paleontological Society Papers*. Lawrence: The Paleontological Society.

Numberger, L., Hemleben, C., Hoffmann, R., Mackensen, A., Schulz, H., Wunderlich, J.-M., & Kučera, M. (2009). Habitats, abundance patterns and isotopic signals of morphotypes of the planktonic foraminifer *Globigerinoides ruber* (d'Orbigny) in the Eastern Mediterranean Sea since the marine isotopic stage 12. *Marine Micropaleontology*, *73*(1–2), 90–104. https://doi.org/10.1016/j.marmicro.2009.07.004

Ohno, Y., Fujita, K., Toyofuku, T., & Nakamaura, T. (2016). Cytological observations of the large symbiotic *foraminifer Amphisorus kudakajimensis* using calcein acetoxymethyl ester. *PLoS ONE*, *11*(11), e0165844. https://doi.org/10.1371/journal.pone.0165844

Osborne, E. B., Thunell, R. C., Marshall, B. J., Holm, J. A., Tappa, E. J., Benitez-Nelson, C., et al. (2016). Calcification of the planktonic Foraminifera *Globigerina bulloides* and carbonate ion concentration: Results from the Santa Barbara Basin. *Paleoceanography*, *31*, 1083–1102. https://doi.org/10.1002/2016PA002933

Pearson, P. N. (2012). Oxygen isotopes in Foraminifera: Overview and historical review. In L. C. Ivany & B. T. Huber (Eds.), *Reconstructing Earth's deep-time climate—The state of the art in 2012, The Paleontological Society Papers* (pp. 1–38). Cambridge: Cambridge University Press.

Peeters, F., Ivanova, E., Conan, S., Brummer, G.-J., Ganssen, G., Troelstra, S., & van Hinte, J. (1999). A size analysis of planktic Foraminifera from the Arabian Sea. *Marine Micropaleontology*, *36*(1), 31–63. https://doi.org/10.1016/S0377-8398(98)00026-7

Pérez, F. F., Gilcoto, M., & Ríos, A. F. (2003). Large and mesoscale variability of the water masses and the deep chlorophyll maximum in the Azores front. *Journal of Geophysical Research*, *108*(C7), 3215. https://doi.org/10.1029/2000JC000360

R Core Team (2019). R: A language and environment for statistical computing. R Foundation for Statistical Computing, Vienna, http://www.R-project.org/

Raitzsch, M., Dueñas-Bohórquez, A., Reichart, G.-J., de Nooijer, L. J., & Bickert, T. (2010). Incorporation of Mg and Sr in calcite of cultured benthic Foraminifera: Impact of calcium concentration and associated calcite saturation state. *Biogeosciences*, *7*, 869–881. https://doi.org/10.5194/bg-7-869-2010

Ravelo, A. C., & Hillaire-Marcel, C. (2007). The use of oxygen and carbon isotopes of Foraminifera in paleoceanography. In C. Hillaire-Marcel, A. de Vernal, & H. Chamley (Eds.), *Proxies in late Cenozoic paleoceanography, Developments in Marine Geology* (pp. 735–764). Amsterdam: Elsevier.

Rebotim, A., Voelker, A. H. L., Jonkers, L., Waniek, J. J., Meggers, H., Schiebel, R., et al. (2017). Factors controlling the depth habitat of planktonic Foraminifera in the subtropical eastern North Atlantic. *Biogeosciences*, *14*, 827–859. https://doi.org/10.5194/bg-14-827-2017

Rebotim, A., Voelker, A. H. L., Jonkers, L., Waniek, J. J., Schulz, M., & Kučera, M. (2019). Calcification depth of deep-dwelling planktonic Foraminifera from the eastern North Atlantic constrained by stable oxygen isotope ratios of shells from stratified plankton tows. *Journal of Micropalaeontology*, *38*(2), 113–131. https://doi.org/10.5194/jm-38-113-2019

Regenberg, M., Nürnberg, D., Steph, S., Groeneveld, J., Garbe-Schönberg, D., Tiedemann, R., & Dullo, W.-C. (2006). Assessing the effect of dissolution on planktonic foraminiferal Mg/Ca ratios: Evidence from Caribbean core tops. *Geochemistry, Geophysics, Geosystems*, *7*, Q07P15. https://doi.org/10.1029/2005GC001019

Reynolds, R. W., Rayner, N. A., Smith, T. M., Stokes, D. C., & Wang, W. (2002). An improved in situ and satellite SST analysis for climate. *Journal of Climate*, *15*, 1609–1625. https://doi.org/10.1175/1520-0442(2002)015<1609:AIISAS>2.0.CO;2

Richey, J. N., Thirumalai, K., Khider, D., Reynolds, C. E., Partin, J. W., & Quinn, T. M. (2019). Considerations *for Globigerinoides ruber* (white and pink) paleoceanography: Comprehensive insights from a long-running sediment trap. *Paleoceanography and Paleoclimatology*, *34*, 353–373. https://doi.org/10.1029/2018PA003417

Rink, S., Kühl, M., Bijma, J., & Spero, H. J. (1998). Microsensor studies of photosynthesis and respiration in the symbiotic foraminifer *Orbulina universa*. *Marine Biology*, *131*, 583–595. https://doi.org/10.1007/s002270050350

Rohling, E. J., & Cooke, S. (2002). Stable oxygen and carbon isotopes in foraminiferal carbonate shells. In B. K. Sen Gupta (Ed.), *Modern Foraminifera* (pp. 240–258). Dordrecht: Kluwer Academic Publishers.

Rohling, E. J., Sprovieri, M., Cane, T., Casford, J. S. L., Cooke, S., Bouloubassi, I., et al. (2004). Reconstructing past planktic foraminiferal habitats using stable isotope data: A case history for Mediterranean Sapropel S5. *Marine Micropaleontology*, *50*, 89–123. https://doi.org/10.1016/S0377-8398(03)00068-9

Rosenthal, Y. (2007). Elemental proxies for reconstructing Cenozoic seawater paleotemperatures from calcareous fossils. In C. Hillaire-Marcel, A. de Vernal, H. Chamley (Eds.), *Proxies in late Cenozoic paleoceanography, Developments in Marine Geology* (pp. 765–797). Amsterdam: Elsevier.

Rosenthal, Y., Oppo, D. W., & Linlsey, B. K. (2003). The amplitude and phasing of climate change during the last deglaciation in the Sulu Sea, western equatorial Pacific. *Geophysical Research Letters*, *30*(8), 1428. https://doi.org/10.1029/2002GL016612

Rousseeuw, P. J., Ruts, I., & Tukey, J. W. (1999). The bagplot: A bivariate boxplot. *The American Statistician*, *53*(4), 382–387. https://doi.org/10.1080/00031305.1999.10474494

Russell, A. D., Hönisch, B., Spero, H. J., & Lea, D. W. (2004). Effects of seawater carbonate ion concentration and temperature on shell U, Mg, and Sr in cultured planktonic Foraminifera. *Geochimica et Cosmochimica Acta*, *68*(21), 4347–4361. https://doi.org/10.1016/j.gca.2004.03.013

Sadekov, A. Y., Darling, K. F., Ishimura, T., Wade, C. M., Kimoto, K., Singh, A. D., et al. (2016). Geochemical imprints of genotypic variants of Globigerina bulloides in the Arabian Sea. *Paleoceanography*, *31*, 1440–1452. https://doi.org/10.1002/2016PA002947

Schiebel, R. (2002). Planktic foraminiferal sedimentation and the marine calcite budget. *Global Biogeochemical Cycles*, *16*(4), 13. https://doi.org/10.1029/2001GB001459

Schiebel, R., Barker, S., Lendt, R., Thomas, H., & Bollmann, J. (2007). Planktic foraminiferal dissolution in the twilight zone. *Deep-Sea Research, Part II: Topical Studies in Oceanography*, *54*(5–7), 676–686. https://doi.org/10.1016/j.dsr2.2007.01.009

Schiebel, R., & Hemleben, C. (2017). *Planktic foraminifers in the modern ocean*. Berlin, Heidelberg: Springer-Verlag.

Schiffelbein, P., & Hills, S. (1984). Direct assessment of stable isotope variability in planktonic Foraminifera populations. *Palaeogeography, Palaeoclimatology, Palaeoecology*, *48*(2–4), 197–213. https://doi.org/10.1016/0031-0182(84)90044-0

Schindelin, J., Arganda-Carreras, I., Frise, E., Kaynig, V., Longair, M., Pietzsch, T., et al. (2012). Fiji: An open-source platform for biological-image analysis. *Nature Methods*, *9*, 676–682. https://doi.org/10.1038/nmeth.2019

Schneider, C. A., Rasband, W. S., & Eliceiri, K. W. (2012). NIH Image to ImageJ: 25 years of image analysis. *Nature Methods*, *9*, 671–675. https://doi.org/10.1038/nmeth.2089

Schweitzer, P. N., & Lohmann, G. P. (1991). Ontogeny and habitat of modern menardiiform planktonic Foraminifera. *Journal of Foraminiferal Research*, *21*(4), 332–346. https://doi.org/10.2113/gsjfr.21.4.332

Shackleton, N. J., Corfield, R. M., & Hall, M. A. (1985). Stable isotope data and the ontogeny of Paleocene planktonic Foraminifera. *Journal of Foraminiferal Research*, *15*(4), 321–336. https://doi.org/10.2113/gsjfr.15.4.321

Siccha, M., & Kučera, M. (2017). ForCenS, a curated database of planktonic Foraminifera census counts in marine surface sediment samples. *Scientific Data*, *4*, 170109. https://doi.org/10.1038/sdata.2017.109

Spero, H. J. (1988). Ultrastructural examination of chamber morphogenesis and biomineralization in the planktonic foraminifer *Orbulina universa*. *Marine Biology*, *99*(1), 9–20. https://doi.org/10.1007/BF00644972

Spero, H. J. (1998). Life history and stable isotope geochemistry of planktonic Foraminifera. In R. D. Norris & R. M. Corfield (Eds.), *Isotope paleobiology and paleoecology, The Paleontological Society Papers* (pp. 7–36). Pittsburgh: The Paleontological Society.

Spero, H. J., Bijma, J., Lea, D. W., & Bemis, B. E. (1997). Effect of seawater carbonate concentration on foraminiferal carbon and oxygen isotopes. *Nature*, *390*, 497–500. https://doi.org/10.1038/37333

Spero, H. J., & Lea, D. W. (1993). Intraspecific stable isotope variability in the planktic Foraminifera *Globigerinoides sacculifer:* Results from laboratory experiments. *Marine Micropaleontology*, *22*, 221–234. https://doi.org/10.1016/0377-8398(93)90045-Y

Spero, H. J., Lerche, I., & Williams, D. F. (1991). Opening the carbon isotope "vital effect" black box: 2. Quantitative model for interpreting foraminiferal carbon isotope data. *Paleoceanography*, *6*(6), 639–655. https://doi.org/10.1029/91PA02022

Spero, H. J., & Williams, D. F. (1988). Extracting environmental information from planktonic foraminiferal δ^{13}C data. *Nature*, *335*, 717–719. https://doi.org/10.1038/335717a0

Spötl, C., & Vennemann, T. W. (2003). Continuous-flow isotope ratio mass spectrometric analysis of carbonate minerals. *Rapid Communications in Mass Spectrometry*, *17*(9), 1004–1006. https://doi.org/10.1002/rcm.1010

Steinhardt, J., Cléroux, C., de Nooijer, L. J., Brummer, G.-J., Zahn, R., Ganssen, G., & Reichart, G.-J. (2015). Reconciling single-chamber Mg/Ca with whole shell δ^{18}O in surface to deep-dwelling planktonic Foraminifera from the Mozambique Channel. *Biogeosciences*, *12*(8), 2411–2429. https://doi.org/10.5194/bg-12-2411-2015

Steinke, S., Chiu, H.-Y., Yu, P.-S., Shen, C.-C., Löwemark, L., Mii, H.-S., & Chen, M.-T. (2005). Mg/Ca ratios of *two Globigerinoides ruber* (white) morphotypes: Implications for reconstructing past tropical/subtropical surface water conditions. *Geochemistry, Geophysics, Geosystems*, *6*, Q11005. https://doi.org/10.1029/2005GC000926

Steph, S., Regenberg, M., Tiedemann, R., Mulitza, S., & Nürnberg, D. (2009). Stable isotopes of planktonic Foraminifera from tropical Atlantic/Caribbean coretops: Implications for reconstructing upper ocean stratification. *Marine Micropaleontology*, *71*, 1–19. https://doi.org/10.1016/j.marmicro.2008.12.004

Thirumalai, K., Richey, J. N., Quinn, T. M., & Poore, R. Z. (2014). *Globigerinoides ruber* morphotypes in the Gulf of Mexico: A test of null hypothesis. *Scientific Reports*, *4*, 6018. https://doi.org/10.1038/srep06018

Toyofuku, T., Matsuo, M. Y., de Nooijer, L. J., Nagai, Y., Kawada, S., Fujita, K., et al. (2017). Proton pumping accompanies calcification in Foraminifera. *Nature Communications*, *8*, 14145. https://doi.org/10.1038/ncomms14145

Ushikawa, J., Penman, D. E., Zachos, J. C., & Zeebe, R. E. (2015). Experimental evidence for kinetic effects on B/Ca in synthetic calcite: Implications for potential $B(OH)_4^-$ and $B(OH)_3$ incorporation. *Geochimica et Cosmochimica Acta*, *150*, 171–191. https://doi.org/10.1016/j.gca.2014.11.022

van Dijk, I., de Nooijer, L. J., Wolthers, M., & Reichart, G.-J. (2017). Impacts of pH and $\left[CO_3^{2-}\right]$ on the incorporation of Zn in foraminiferal calcite. *Geochimica et Cosmochimica Acta*, *197*, 263–277. https://doi.org/10.1016/j.gca.2016.10.031

van Eijden, A. J. M. (1995). Morphology and relative frequency of planktic foraminiferal species in relation to oxygen isotopically inferred depth habitats. *Palaeogeography, Palaeoclimatology, Palaeoecology*, *113*, 267–301. https://doi.org/10.1016/0031-0182(95)00057-S

Vetter, L., Kozdon, R., Mora, C. I., Eggins, S. M., Valley, J. W., Hönisch, B., & Spero, H. J. (2013). Micron-scale intrashell oxygen isotope variation in cultured planktic foraminifers. *Geochimica et Cosmochimica Acta*, *107*, 267–278. https://doi.org/10.1016/j.gca.2012.12.046

Wagenmakers, E.-J., & Farrell, S. (2004). AIC model selection using Akaike weights. *Psychonomic Bulletin & Review*, *11*(1), 192–196. https://doi.org/10.3758/BF03206482

Wang, L. (2000). Isotopic signals in two morphotypes of *Globigerinoides ruber* (white) from the South China Sea: Implications for monsoon climate change during the last glacial cycle. *Palaeogeography, Palaeoclimatology, Palaeoecology*, *161*(3–4), 381–394. https://doi.org/10.1016/S0031-0182(00)00094-8

Waniek, J., Koeve, W., & Prien, R. D. (2000). Trajectories of sinking particles and the catchment areas above sediment traps in the northeast Atlantic. *Journal of Marine Research*, *58*(6), 983–1006. https://doi.org/10.1357/002224000763485773

Waniek, J. J., Schulz-Bull, D. E., Blanz, T., Prien, R. D., Oschlies, A., & Müller, T. J. (2005). Interannual variability of deep water particle flux in relation to production and lateral sources in the northeast Atlantic. *Deep-Sea Research, Part I: Oceanographic Research Papers*, *52*(1), 33–50. https://doi.org/10.1016/j.dsr.2004.08.008

Watson, E. B. (2004). A conceptual model for near-surface kinetic controls on the trace-element and stable isotope composition of abiogenic calcite crystals. *Geochimica et Cosmochimica Acta*, *68*(7), 1473–1488. https://doi.org/10.1016/j.gca.2003.10.003

Weiner, A., Aurahs, R., Kurasawa, A., Kitazato, H., & Kučera, M. (2012). Vertical niche partitioning between cryptic sibling species of a cosmopolitan marine planktonic protist. *Molecular Ecology*, *21*(16), 4063–4073. https://doi.org/10.1111/j.1365-294X.2012.05686.x

Weinkauf, M. F. G., Groeneveld, J., Waniek, J. J., Vennemann, T., & Martini, R. (2020). Shell morphology and geochemistry of *Globigerinoides ruber*/*elongatus* from sediment trap Kiel 276-25 (May 2005–March 2006). https://doi.org/10.6084/m9.figshare.12090630

Weinkauf, M. F. G., Kunze, J. G., Waniek, J. J., & Kučera, M. (2016). Seasonal variation in shell calcification of planktonic Foraminifera in the NE Atlantic reveals species-specific response to temperature, productivity, and optimum growth conditions. *PLoS ONE*, *11*(2), e148363. https://doi.org/10.1371/journal.pone.0148363

Weinkauf, M. F. G., Moller, T., Koch, M. C., & Kučera, M. (2013). Calcification intensity in planktonic Foraminifera reflects ambient conditions irrespective of environmental stress. *Biogeosciences*, *10*(10), 6639–6655. https://doi.org/10.5194/bg-10-6639-2013

Weinkauf, M. F. G., Zwick, M. M., & Kučera, M. (2020). Constraining the role of shell porosity in the regulation of shell calcification intensity in the modern planktonic foraminifer *Orbulina universa* d'Orbigny. *Journal of Foraminiferal Research*, *50*(2), 195–203. https://doi.org/10.2113/gsjfr.50.2.195

Wit, J. C., Reichart, G.-J., & Ganssen, G. M. (2013). Unmixing of stable isotope signals using single specimen $\delta^{18}O$ analyses. *Geochemistry, Geophysics, Geosystems*, *14*, 1312–1320. https://doi.org/10.1002/ggge.20101

Yu, J., Day, J., Greaves, M., & Elderfield, H. (2018). Determination of multiple element/calcium ratios in foraminiferal calcite by quadrupole ICP-MS. *Geochemistry, Geophysics, Geosystems*, *6*, Q08P01. https://doi.org/10.1029/2005GC000964

Zarkogiannis, S. D., Antonarakou, A., Tripati, A., Kontakiotis, G., Mortyn, P. G., Drinia, H., & Greaves, M. (2019). Influence of surface ocean density on planktonic Foraminifera calcification. *Scientific Reports*, *9*, 533. https://doi.org/10.1038/s41598-018-36935-7

Zeebe, R. E., Bijma, J., Hönisch, B., Sanyal, A., Spero, H. J., & Wolf-Gladrow, D. A. (2008). Vital effects and beyond: A modelling perspective on developing palaeoceanographical proxy relationships in Foraminifera. In W. E. N. Austin & R. H. James (Eds.), *Biogeochemical controls on palaeoceanographic environmental proxies, Geological Society Special Publications* (pp. 45–58). London: The Geological Society.

Zweng, M. M., Reagan, J. R., Seidov, D., Boyer, T. P., Locarnini, R. A., Garcia, H. E., et al. (2018). Salinity. In A. Mishonov (Ed.), *World Ocean Atlas 2018, NOAA Atlas NESDIS* (Vol. 2, pp. 1–40). Silver Spring: National Oceanic and Atmospheric Administration.